

# Defective Metal-Organic Frameworks

Stefano Dissegna, Konstantin Epp, Werner R. Heinz, Gregor Kieslich,\*  
and Roland A. Fischer\*

The targeted incorporation of defects into crystalline matter allows for the manipulation of many properties and has led to relevant discoveries for optimized and even novel technological applications of materials. It is therefore exciting to see that defects are now recognized to be similarly useful in tailoring properties of metal-organic frameworks (MOFs). For instance, heterogeneous catalysis crucially depends on the number of active catalytic sites as well as on diffusion limitations. By the incorporation of missing linker and missing node defects into MOFs, both parameters can be accessed, improving the catalytic properties. Furthermore, the creation of defects allows for adding properties such as electronic conductivity, which are inherently absent in the parent MOFs. Herein, progress of the rapidly evolving field of the past two years is overviewed, putting a focus on properties that are altered by the incorporation and even tailoring of defects in MOFs. A brief account is also given on the emerging quantitative understanding of defects and heterogeneity in MOFs based on scale-bridging computational modeling and simulations.

## 1. Introduction

Defects in crystalline materials have fascinated scientists since the very beginning of crystal chemistry and materials science.<sup>[1]</sup> The arguably most stunning example that originates from the elaborate control of *defect chemistry* are doped semiconductors, forming the foundation of pn junctions that are used in many devices.<sup>[2]</sup> Other fascinating examples are cuprates such as  $\text{YBa}_2\text{Cu}_3\text{O}_{7-x}$ , in which the level of oxygen deficiency determines the temperature where these materials become superconducting.<sup>[3]</sup> Structurally more complex cases include materials such as  $\text{Fe}_{1-x}\text{O}$  and so-called Magnéli phases, where the occurrence of oxygen defects lead to new structure motifs,<sup>[4]</sup> that is, ordered vacancies in  $\text{Fe}_{1-x}\text{O}$  and the occurrence of shear structures (Wadsley defects) in compounds such as  $\text{Ti}_5\text{O}_9$ ,  $\text{V}_6\text{O}_{11}$ , or  $\text{W}_{10}\text{O}_{29}$ .<sup>[5]</sup> Imperfections such as point defects naturally occur at temperatures above 0 K; however, it is the artificial control of the defect concentration, the so-called *defect engineering*, that allows us to alter a certain property by the incorporation of


defects into a parent framework. Having this remarkable history in mind, we can summarize that the control of defect structure and chemistry is an additional lever—a dimension beyond compositional distinction and structural perfection—that scientists have in hand to alter properties of a parent compound. It therefore seems only natural that defects have now been recognized to be similarly useful in tuning properties of metal-organic frameworks (MOFs).<sup>[6]</sup>

Before focusing on the defect chemistry and the functions coming with them, it is important to stress that MOFs, formally a subclass of porous coordination polymers, are a unique family of materials, merging the rich Werner-type coordination and cluster chemistry with the parameter space of organic chemistry. By combining organic chemistry and coordination chemistry on a molecular level with

crystal chemistry and the large opportunities that come with postsynthetic treatment (PST) methods,<sup>[7,8]</sup> MOFs *have changed our perception of crystalline materials*, as recently highlighted by Ohrström.<sup>[9]</sup> There are numerous parameters scientists have in hand for a guided synthesis, such as the reticular chemistry approach,<sup>[10]</sup> which combined with a clever choice of linker molecules and defined metal ion nodes (“bricks”), enables us to design porosity, surface chemistry, and the functionalization of the coordination space in a new fashion. At the same time, the large parameter space challenges chemists, and elaborate structure–property relations are only being developed gradually. In turn, MOFs cover a broad range of fascinating properties and raised and still raise the interest of many scientists with various backgrounds, thereby crossing boundaries of traditional scientific disciplines.

Since our last review in 2014,<sup>[6]</sup> a lot has happened which fits under the umbrella of *defective MOFs* as a key word. In particular, we would like to highlight the several reviews and perspective essays that appeared on the topic of disorder and heterogeneity in inorganic–organic frameworks, emphasizing the link between configurational disorder, defects, and entropy in MOFs.<sup>[11–13]</sup> When looking back, a true milestone in the field has been the work by Cliffe et al. in 2014,<sup>[14]</sup> observing defect ordering in UiO-66 (Universitetet i Oslo) into nanoregions of *reo* topology. Although we have discussed their work in our last review, it is only now that the impact of their results has become clear and hence UiO-66 has developed to the model system when dealing with defective MOFs. Their work depicts one of the rare experimental in-depth and rigorous structural

S. Dissegna, K. Epp, W. R. Heinz, Dr. G. Kieslich, Prof. R. A. Fischer  
Chair of Inorganic and Metal-Organic Chemistry  
Department of Chemistry  
Technical University of Munich  
Lichtenbergstraße 4, 85748 Garching, Germany  
E-mail: Gregor.Kieslich@tum.de; Roland.Fischer@tum.de

 The ORCID identification number(s) for the author(s) of this article can be found under <https://doi.org/10.1002/adma.201704501>.

DOI: 10.1002/adma.201704501

study on defective MOFs<sup>[14]</sup> and further highlights the close relation to defects in inorganic materials, e.g., that order phenomena of defects can lead to structure motifs different from the parent phase. The results inspired many following studies and at the same time raise the flag for the need of high-quality structural investigations on defective MOFs, based on both advanced experimental and computational simulation and modeling techniques. Presently, we observe that research in the area of defect characterization and in turn defect engineering of MOFs is empirical and function-driven, while only a few studies exist which focus on an elucidation of detailed structure–property relations guided by an atomistic and mesoscopic level of quantitative understanding. From this viewpoint it is clear that *defect engineering in MOFs*, in which the targeted incorporation of defects is used to introduce or alter a certain property, depicts a most challenging research goal rather than a current state of art. The aim of this review is to critically update the reader about the recent progress in the field and the focus is put on (new) properties arising from defects and the ability to tune these.

## 1.2. What is a Defect?

Before discussing research trends within the area of the past two years in more detail, we like to address the general definition of a defect. Here, we like to follow on from our previous work, defects being “*sites that locally break the regular periodic arrangement of atoms or ions of the crystalline parent framework because of missing or dislocated atoms or ions.*”<sup>[6]</sup> When applying this definition on MOFs, dynamic disorder coming from substituents at the linkers, dangling side chains for example, is explicitly excluded. It is also worth noting that defect structure of the crystallite external surface is excluded, which of course is the largest irregularity when looking at materials on the nanoscale. Additionally, it is possible to further define subclasses of defects such as point defects, line defects, and planar defects.<sup>[1]</sup> The latter two are mainly of fundamental interest and their influence on properties in MOFs has yet not been of intensive focus.<sup>[15]</sup> Following on from our definition, it is also important to mention that the infiltration of a parent MOF by coordinating chemically noninnocent guests, e.g., the gas or liquid loading of 7,7,8,8-tetracyanoquinodimethan (TCNQ) into pores of HKUST-1 (Hong Kong University of Science and Technology),<sup>[16]</sup> creates a defective system. This can be further rationalized by looking at the cubic symmetry of HKUST-1. By infiltration of TNCQ, two uncoordinated metal sites in HKUST-1 are bridged and a second coordination network is formed within the parent structure, thereby breaking the cubic symmetry of the parent framework. Hence, we will pick up on this system in context of electronic transport in MOFs.

After defining a defect in a general way, it is now important to define a common language that not only is scientifically sound, but at the same time presents an intuitive basis for discussion. Within the field of MOFs, the most important point defects are (i) missing linker defects, (ii) missing node defects, (iii) modified node defects, and (iv) modified linker defects. It is important to realize that a missing node defect is a result of a critical concentration and spatial distribution of missing linker defects,



**Gregor Kieslich** is an inorganic chemist focusing on crystal chemistry and structure–property relations in functional solids and hybrid frameworks. He studied chemistry between 2006 and 2010 at the Johannes Gutenberg University in Mainz. After completing his PhD in 2013 with Prof. W. Tremel, he moved to Cambridge University to work with Prof. A. K. Cheetham. Throughout his career he has been awarded several fellowships, including the Konrad–Adenauer PhD fellowship and the DFG research fellowship. Since August 2016, he has been a Junior Research Group leader at the Technical University of Munich, holding a Liebig-Fellowship.



**Roland A. Fischer** received his Dr. rer. nat. in 1989 and Habilitation in 1995 from Technical University Munich (TUM). He was Associate Professor at Heidelberg University (1996–1997) and Full Professor for Inorganic Chemistry at Ruhr-University Bochum (1997–2015). In 2016, he returned to TUM and took the Chair of Inorganic and Metal-Organic Chemistry. He was elected Vice President of the Deutsche Forschungsgemeinschaft (DFG) in 2016. His research focuses on main group 13/transition metal compounds and clusters, precursors for metal-organic chemical vapor deposition (MOCVD), and the materials chemistry of metal-organic frameworks (MOFs).

or in other words it is the result of an unequal distribution of linker defects within the framework. It is similarly important to realize that the equilibrium between those two, missing linker and missing node defects, is extremely difficult to tell, and in the most cases, only indirectly accessible. In that sense, UiO-66 depicts an exception where it seems to be energetically favorable, not only to create missing nodes, but further create these in close vicinity of each other to build *revo* nanoregions that in turn can directly be detected by X-ray diffraction (XRD) methods.<sup>[14,17]</sup> In most cases, however, such an ordering is not observed (yet) and scientists must rely on indirect methods, e.g., the analysis of the Brunauer–Emmet–Teller (BET) surface area in combination with results from thermogravimetric analysis (TGA) and a range of spectroscopic evidences. Therefore, when discussing defects in the text, we follow the suggestions by the authors of the original publication, e.g., in the assignment and discussion which type of defects have been formed. Similar conclusions can be drawn for the heterogeneity introduced by modified nodes and linker defects, which might be accessible by X-ray nanotomography in the future.

Broadly, the intentional incorporation of defects and the subsequent application of defective MOFs as heterogeneous catalysts

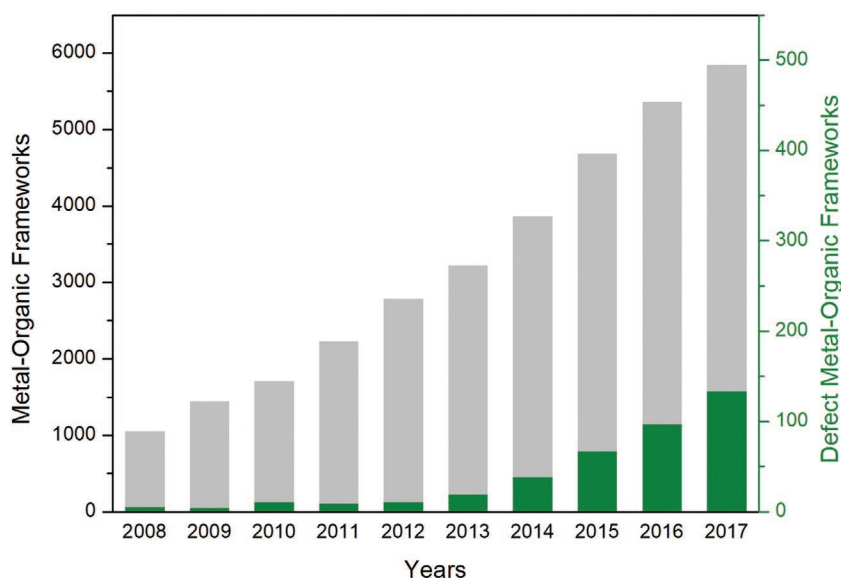


**Figure 1.** Total number of publications on the topic over the past decade. The plot was created based on entries in the Web of Science (31 June 2017) by using the keywords “metal-organic frameworks” (gray) and “defect metal-organic frameworks” (green).

simulation techniques use periodic boundary conditions, which make the explicit treatment of defect sites and their distribution challenging. In principle, choosing a large enough starting unit could account for disorder, but practically the size of this unit is constrained by computational demands. However, there are scale-bridging approaches to circumvent such difficulties and in turn calculate properties such as gas sorption and mechanical properties in dependency of defect incorporation.<sup>[23]</sup> At this point it is already evident that defect chemistry of MOFs offers a great deal of opportunities for the targeted manipulation of various properties. Although extremely challenging, the rising interest of scientists and the related increase of publications on this topic are self-evident (see **Figure 1**). In the following chapters, we review the trends and developments in detail, focusing on the properties of defective MOFs that have been studied over the course of the past two years.

is one of the largest area of research today. The creation of linker defects that introduce *Lewis* acidic sites together with missing node defects that reduce diffusion limitations of products and educts offers particularly fascinating opportunities. Catalytic reactions with defective MOFs that have been successfully tested are the dimerization of ethylene and the cyanosilylation of benzaldehyde.<sup>[18,19]</sup> It is important to have in mind, however, that established catalysts still outperform defective MOFs as they would outperform “perfect” MOFs and are reasonably cheap at the same time.<sup>[20]</sup> Thus, potential applications of (defective) MOFs still seem to be limited to the field of fine chemical catalysis. In this context, it is no surprise that research focus has also been drawn on the chemical manipulation of the inner framework, e.g., by the introduction of different linker functionalities<sup>[21]</sup> or modification of the metal node.<sup>[22]</sup> These manipulations allows for accessing the factors such as the hydrophilicity of the framework and access to reactive sites and expanded coordination space in proximity of reactive centers. At the same time, computational scientists also entered the field. However, standard

## 2. Synthesis and Characterization of Defects

The targeted incorporation of defects into MOFs, i.e., the synthetic control of defect concentration and chemical nature of defect, remains challenging until today. We can distinguish between two synthetic routes that have been applied in the recent literature for the preparation of MOFs with various types of defects: (i) the “de novo” synthesis and (ii) the use of post-synthetic treatment methods. A schematic representation of all applied methods to create defects in MOFs is given in **Figure 2**. We briefly like to remind the reader about the general procedure of the two methods and the underlying chemistry; however, for a more detailed discussion we refer to our previous review.<sup>[6]</sup>

### 2.1. De Novo Synthesis of Defects

To date, the most common approach in the community for the synthesis of defective MOFs is the addition of large amounts

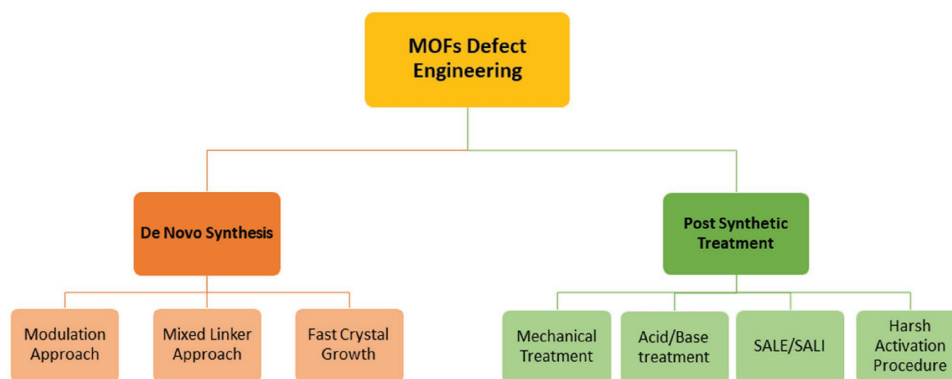


**Figure 2.** Representation of all main procedures to create defects in MOFs.

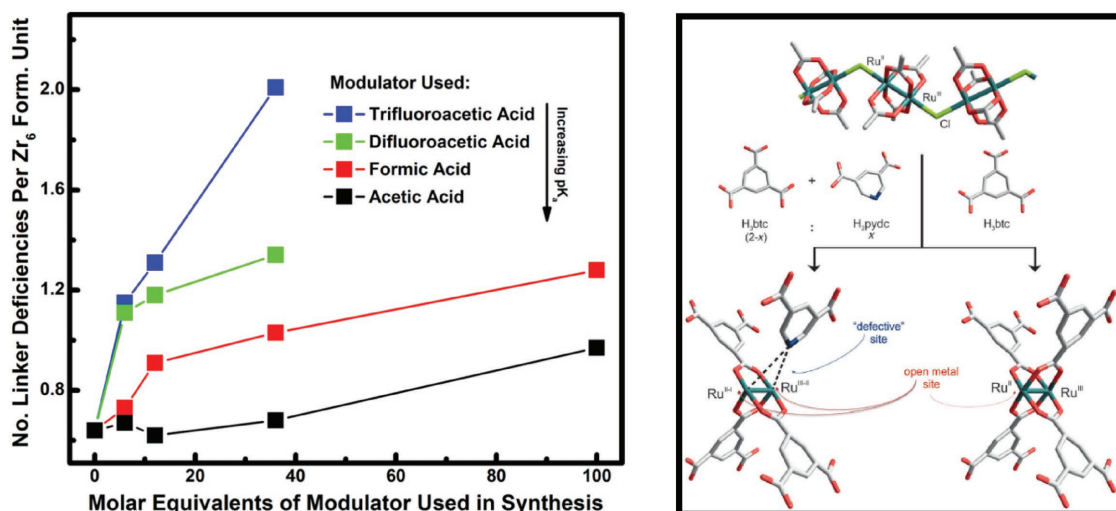


**Figure 3.** Left panel: Plot of the amount of linker deficiencies per Zr<sub>6</sub> formula unit against the molar equivalents of modulator in UiO-66. Reproduced with permission.<sup>[17]</sup> Copyright 2016, American Chemical Society. Right panel: Mixed linker approach in Ru-HKUST-1 leads to modified node defects. Reproduced with permission.<sup>[25]</sup> Copyright 2014, John Wiley & Sons.

of monocarboxylic acids in addition to the linker molecules during the MOF synthesis. This approach, known as *modulation approach*, originates from the synthetic attempts of reducing crystallization speed of MOFs to obtain higher degrees of crystallinity. It is established today that small amounts of monocarboxylic acids, the so-called modulator, slow down the speed of crystallization by impacting the equilibrium reaction—the formation of the framework—while large modulator concentrations facilitate the built-in of these and in turn the formation of defects. The first report using this approach is given by Ravon et al. in 2010, who used 2-methyl-toluic acid as modulator in the synthesis of MOF-5.<sup>[24]</sup> Since then, many research groups focused on the synthesis of defective MOFs, with typical modulators being formic acid (FA), acetic acid (AA), trifluoroacetic acid (TFA), difluoroacetic acid (DFA), and their derivatives (see Figure 3, left panel).

In 2013, Vermoortele et al. applied the modulator approach to produce highly defective UiO-66, by using TFA as modulator.<sup>[26]</sup> In their work, the authors subsequently removed TFA by thermal treatment at 320 °C, creating unsaturated sites as highly reactive *Lewis* acid sites that implicate the application of such systems in catalysis. It was only in 2016 when Shearer et al. systematically studied the impact of different modulators such as FA, AA, TFA, and DFA on the defect chemistry of UiO-66.<sup>[17]</sup> The authors observed a correlation between the defect concentration and the *Brønsted* acidity of the modulator. Therewith, based on its pK<sub>a</sub> (which is solvent dependent) TFA appears to be the most suitable modulator of the above series for the synthesis of defective UiO-66. It is worth noting that so far research has focused on applying the modulator approach to MOFs with carboxylic acids as linkers, with UiO-66 currently being the model system for many studies.

In the so-called mixed linker approach, the linker of the parent framework is partially substituted by a linker with having a different coordinating group, e.g., 1,3,5-tricarboxylate (BTC<sup>3-</sup>) by pyridine-3,5-dicarboxylate (pydc<sup>2-</sup>).<sup>[27]</sup> An example for this approach is depicted in Figure 3 (right panel), which shows the

work of Kozachuk et al. based on Ru-HKUST-1. They find a formal reduction of the Ru centers, induced by the reaction conditions.<sup>[25]</sup> Following the impact of the modulator on the reaction kinetics and crystallinity of MOFs, it is intuitive that a fast crystallization process similarly leads to the formation of point defects, e.g., missing linker or missing cluster defects. Reaction processes to facilitate a fast crystallization include microwave-assisted synthesis as well as high concentration of the precursors. Point defects created by this approach can then be replaced by other species (counter anions) present in the MOF mother solution to further increase the functionality, e.g., OH groups in MOF-5 and IRMOF-3 (isorecticular metal-organic framework).<sup>[28]</sup>

## 2.2. Defects Created by Postsynthetic Treatment

The second synthetic approach toward defective MOFs involves the introduction of defect sites after the synthesis of the parent MOF, hence it is termed *postsynthetic treatment*. There exist several variations of which all involve a heterogeneous treatment of the parent MOF with modified linkers or acids. For instance, Vermoortele et al. used strong acids such as HClO<sub>4</sub> and TFA for the postsynthetic modification of MIL-100 (Fe) (Material of the Institute Lavoisier).<sup>[29]</sup> The authors observe the formation of additional *Brønsted* acid sites in close vicinity to the *Lewis* acidic sites, the existence of which was proven by CO chemisorption experiments. Furthermore, no loss in crystallinity was observed after this treatment; however, the authors found a decrease in porosity which was ascribed to the presence of larger counteranions such as ClO<sub>4</sub><sup>-</sup> and/or disconnected ligands within the pores.

The arguably most established postsynthetic treatment method is the so-called “solvent-assisted ligand exchange” (SALE). Briefly, SALE (see Figure 4) involves the replacement of linkers in an MOF with modified linkers of choice, e.g., functionalized<sup>[30]</sup> or longer linker,<sup>[30]</sup> or linker with an incorporated catalyst precursor,<sup>[31]</sup> via a heterogeneous reaction in a selected solvent. Importantly, SALE facilitates the synthesis of MOFs



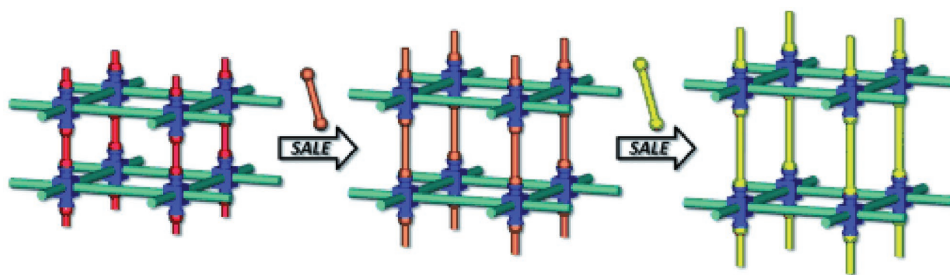


**Figure 4.** Schematic representation of postsynthetic linker exchange with SALE. Reproduced with permission.<sup>[32]</sup> Copyright 2014, John Wiley & Sons.

that are difficult to obtain with a mixed linker approach, e.g., NU-125-HBTC (NU = Northwestern University).<sup>[31,33]</sup> In general, it can be summarized that SALE is particularly useful in the modification of very stable MOFs with high coordination numbers such as UiO-66 and also zeolitic imidazolate framework (ZIFs). Stuningly, Karagiari et al.<sup>[31]</sup> reported the successful replacement of 85% of the linkers (methylimidazole) in ZIF-8 with imidazole, resulting in a material with increased pore openings that allow bulkier molecules to react with the coordinatively unsaturated sites (CUS) present in the system. Similar to the *de novo* approach reported by Kozachuck et al., SALE also enables the introduction of linkers with different coordination sites, thereby modifying the electronic state of the metal node. Additionally, there are reports where MOF ligands are exchanged by solvent molecules itself (DMF) due to the ability of the solvent to coordinate to CUS as shown by Lee et al.<sup>[34]</sup> Likewise, the solvent-assisted ligand incorporation (SALI) allows for manipulating the functionality of the metal node with leaving the linker of the framework untouched.<sup>[35]</sup> For instance, Deria et al. used different perfluorinated carboxylic acids coordinating to vacant sites at the node to increase the hydrophobicity of NU-1000 and its CO<sub>2</sub> capture ability. As described by Deria et al., this new postsynthetic technique relies on acid–base chemistry between the hydroxyl groups on the NU-1000 node and the carboxylate group of the perfluorinated chain.

Moreover, extensive washing and harsh activation procedures (especially high temperatures) can produce significant amounts of defects, likely coming from hydrolysis reactions as suggested by Shearer et al.<sup>[36]</sup> In MOF-5, thermal treatment can induce the *in situ* decarboxylation of terephthalic acid, generating linker fragments postsynthetically.<sup>[37]</sup> The main advantage is the simple synthetic procedure; however, a systematic control of defect creation is very difficult due to its intrinsic low reproducibility. Last but not less important, Bennett et al. used ball milling to gradually destroy UiO-66, MIL-140, and MIL-140b frameworks by the breaking of a fraction of metal–ligand bonds. Interestingly, the inorganic Zr<sub>6</sub>O<sub>4</sub>(OH)<sub>4</sub> clusters of UiO-66 remain intact while the MILs ZrO chains undergo a substantial distortion.<sup>[38]</sup>

### 2.3. Characterization of Defects

The in-depth characterization of defects, e.g., the elucidation of defect concentration and spatial distribution, as well as the defect chemistry as a function of both parameters challenges

common characterization techniques. For instance, laboratory X-ray diffraction relies on the periodic arrangement of the lattice and only minor changes, oftentimes beyond the resolution of lab X-ray techniques, are expected in the Bragg diffraction pattern of defective MOFs. In contrast to that, experimental techniques that can probe the local structure, e.g., the analysis of the pair distribution function (PDF) or the extended X-ray absorption fine structure (EXAFS), can be used. Such techniques, however, require the use of synchrotron sources and usually go beyond common laboratory techniques; hence, our structural insight into defects and heterogeneity in MOFs is yet limited. The study by Cliffe et al. from 2014 depicts one of the rare examples, where a combination of several techniques such as (anomalous) powder X-ray diffraction (PXRD) and PDF combined with computational modeling was used to access the defect chemistry of UiO-66.<sup>[14]</sup> On the basis of their results (and the insight the authors provide), it is no surprise that UiO-66 is presently the model framework within the field. Particularly, the formation of nanoregions with *reo* topology in UiO-66, which come with small intensities in the PXRD pattern, have sharpened our perception when analyzing PXRD data related to defective MOFs.

Inspired by their study, Shearer et al. have systematically studied defective UiO-66 by applying several different characterization techniques such as PXRD, BET (N<sub>2</sub> physisorption), and high-resolution nuclear magnetic resonance (NMR) after digesting the defective MOF. They found a correlation between modulator used and the amount of *reo* nanoregions in defective UiO-66 (see Figure 3 (left panel) and Figure 5).<sup>[17]</sup> Similarly, Atzori et al. recently reported on the specific influence of benzoic acid modulation toward the formation of missing cluster defects.<sup>[39]</sup> It is important to emphasize that the method, in particular the use of lab PXRD, is yet limited to UiO-66 derivatives since the occurrence of correlated defect nanoregions has only been found for UiO-66. Other common characterization techniques in the field such as N<sub>2</sub> physisorption, Fourier transform infrared spectroscopy, or TGA can be used to screen a property that will be affected by defects; however, as the structure is not explicitly screened, the application and subsequent analysis of only one method can be misleading. Therefore, it is necessary to apply an orchestra of indirect characterization techniques. For instance, TGA coupled mass spectrometry can provide insightful information into the overall composition; however, one could also envision that a modulator can similarly act as capping agent being on the external surface of the MOF crystallite. In the occasion of MOF particles in the nanoregime, this amount can

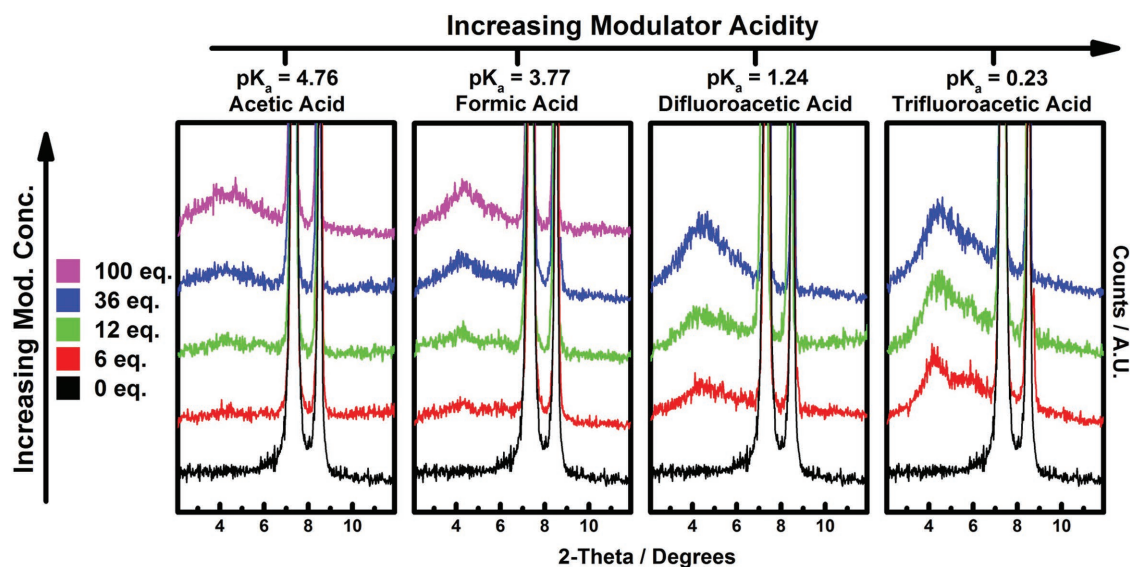


**Figure 5.** Influence of amount and type of different monocarboxylic acid modulators on the low-angle region in the respective PXRD patterns of UiO-66 samples. Reproduced with permission.<sup>[17]</sup> Copyright 2016, American Chemical Society.

be significant in comparison to the overall amount of linkers. Following the developments of the field over the past years, we here focus on less common characterization techniques that have been applied over the course of the past two years that, from our perspective, are expected to be promising for future developments in the field.<sup>[40–42]</sup>

A fascinating technique that recently found its way to the field of MOF is the use of positrons as probe of porosity, namely positron annihilation lifetime spectroscopy (PALS). Positrons (Ps), the antiparticles of electrons, annihilate by the interaction with electrons under the release of gamma rays that can be detected. In an MOF, the main electron density is located at the framework, coupling the Ps lifetime to the pore size. Since PALS can be performed in situ, it is possible to follow the pore size evolution during materials synthesis. In core–shell particles, for example, where the surface of a porous material is covered with a dense, nonpermeable layer, N<sub>2</sub> physisorption analysis is at its limits. Already in 2010, Liu et al. have applied PALS to MOFs for the first time.<sup>[43,44]</sup> In essence, they assigned the shape of the micropores, found incomplete pore filling with CO<sub>2</sub> at high pressures, and detected a small fraction of mesoporosity (i.e., clustered missing node defects) which was below detection limits of standard N<sub>2</sub> physisorption analysis.<sup>[43,44]</sup>

In 2016, Mondal et al. applied PALS to study mesopores in hydrogen-bonded imidazolate framework (HIF-3).<sup>[45]</sup> The authors assigned missing building blocks in HIF-3 as reason for mesopores that are responsible for structural flexibility during gas uptake. PALS may be applied more often in the future since it enables pore size determinations during synthesis. Furthermore, an in-depth understanding on the formation of mesopores as a function of reaction time or even during the heating phase of a reaction is still an open question. Thornton et al. have also applied PALS for the characterization of a metal-organic glass formed by melt quenching of ZIF-4. It shows an intermediate porosity between the pristine, open ZIF-4, and

the densified ZIF-zni. Among the three materials, only pristine ZIF-4 porosity is accessible for nitrogen adsorption.<sup>[46]</sup>

Potentiometric acid–base titration is another useful technique that gives insight to the chemistry of defects in MOFs. In more detail, potentiometric titration makes the quantification and differentiation between distinct *Bronsted* sites and their pK<sub>a</sub> values possible. Klet et al. investigated several Zr-based MOFs such as UiO-66, MOF-808, and NU-1000.<sup>[47,48]</sup> With UiO-66 (Zr and Hf) for instance, they obtained titration curves displaying three inflection points (see **Figure 6**, left panel). Three different pK<sub>a</sub> values were determined and assigned not only to the μ<sup>3</sup>-OH groups already present in “defect-free” UiO-66 but also to the values matching the acidity of metal-bound hydroxo and aqua ligands. The authors assumed that the occurrence of these species originates from missing linker defects (see **Figure 6**, right panel).<sup>[48]</sup>

In comparison to commonly used TGA, potentiometric acid–base titration is not sensitive toward typical TGA-related conflicting issues such as inconclusive on- and offset temperatures, the formation of nonvolatile carbonaceous products, or incomplete activation procedures.<sup>[49]</sup> However, potentiometric titrations have practical issues too. For example, inconsistent reproducibility and challenging data interpretation, for similar pK<sub>a</sub> values, flat titration curves, and diffusion limitations, may be of concern. Furthermore, a high stability of the MOF toward acids and bases is a prerequisite for the measurement and limits its applicability.<sup>[49]</sup>

Water adsorption measurement is another useful technique to access the chemistry of defects in porous materials such as zeolites and MOFs.<sup>[6]</sup> As described by Canivet et al.,<sup>[50]</sup> this technique can be rationalized using a simple set of parameters: the Henry constant (which is the slope of the adsorption pressure in the low pressure range), the pressure at which pore filling occurs, and the maximum water adsorption capacity. The first two parameters are correlated, both containing information on the hydrophilicity of the

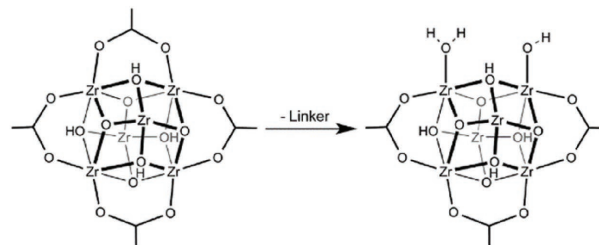
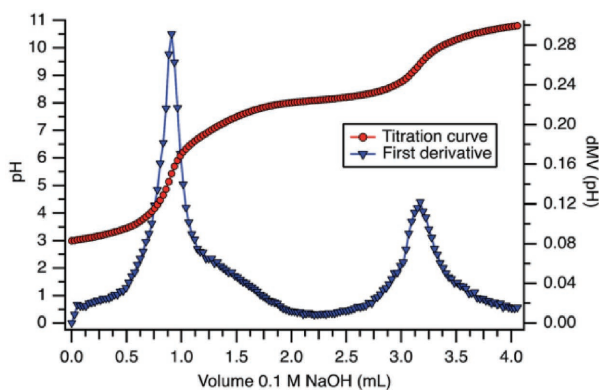


**Figure 6.** Left panel: Titration curve (red) and its first derivative (blue) from an Hf-UiO-66 sample. Right panel: Missing linker defects as reason for M–OH<sub>2</sub> and M–OH groups. Reproduced with permission.<sup>[47]</sup> Copyright 2016, The Royal Society of Chemistry.

material.<sup>[51]</sup> These parameters, as shown by Dissegna et al., can be used to access the chemistry of CUS in UiO-66.<sup>[19]</sup> As expected, an increase of defective sites in UiO-66 leads to an increase in both hydrophilicity and the maximum water capacity. Both were then correlated with an increased activity in a *Lewis* acid catalyzed reaction. Furthermore, the linker functionalization of the material by hydrogen bonding groups such as amine or aldehyde systematically leads to an increase in the *Henry* constant and comes with a decrease in the pore filling pressure.

### 3. Function and Properties of MOFs

The incorporation of defects into MOFs gives researchers an additional set of parameters for tuning properties such as (micro)porosity, active catalytic sites, among others. Moreover, there are even properties, such as charge transport, that may only exist in defective MOFs and are absent in the respective parent framework. In the following paragraph, we discuss the most important discoveries of the past two years.

#### 3.1. Catalysis

MOFs with their porosity and available *Lewis* acidic sites implicate the application of these in heterogeneous catalysis. Consequently, much focus was put on the application of MOFs in catalysis over the recent years, especially of how the introduction of defects can improve the performance of a parent MOF in heterogeneous catalysis. The overall goal in this research area is—and must be—the establishment of structure–property relations on an atomic level, whereby it is envisioned that structural manipulation of active sites leads to direct changes in the catalytic reactivity.

Recently, Hupp and co-workers reported on the correlation of defects and catalytic activity, whereby the acid-catalyzed epoxide ring opening of styrene oxide was examined as a test reaction.<sup>[48]</sup> They studied a series of Zr/Hf-based MOFs, namely UiO-66, UiO-67, PCN-57 (porous coordination network), NU-1000, and MOF-808, exploring the number of defects by using potentiometric titration. The authors showed that the

catalytic activity can be attributed to defective sites and/or the connectivity of the Zr<sub>6</sub>/Hf<sub>6</sub>-clusters. Interestingly, defect-free Zr-UiO-67 exhibits almost no catalytic conversion, while defective Zr-UiO-67 (HCl as modulator) with 1.75 missing Linkers per Zr<sub>6</sub> cluster shows a catalytic conversion of ≈40% after 24 h. Moreover, NU-1000 and MOF-808 were found to be significantly more active catalysts due to their intrinsic lower connectivity of 8 and 6 Linkers per Zr<sub>6</sub> cluster and more exposed Zr<sub>6</sub>-nodes bearing additional –OH/–H<sub>2</sub>O groups. Notably, there is a conceptual difference in engineered defects using modulators and as proposed by the authors “inherent defects” that are defined as deviations from the fully coordinated Zr<sub>6</sub> clusters (12 linkers per Zr<sub>6</sub> cluster) with lowered connectivity (8 or 6 linkers per Zr<sub>6</sub> cluster). Other good examples of how the catalytic activity of a parent MOF can be enhanced depicts the dimerization of ethylene and Paal–Knorr reaction.<sup>[52]</sup> Zhang et al. applied the solid solution approach in ruthenium analogs of [Cu<sub>3</sub>(btc)<sub>2</sub>]<sub>n</sub> (HKUST-1), Ru-MOF, in which ditopic isophthalate was used as defect-generating linker, creating modified node defects. By using ditopic instead of tritopic linkers, undercoordinated and formally Ru<sup>δ+</sup> sites were obtained, which can act as soft *Lewis* acid sites. In the dimerization of ethylene the defect engineered Ru-MOF sample containing 32% of 5-OH-ip (5-hydroxy-isophthalate) linker revealed a twofold increase in the turnover frequency, when compared to the parent Ru-MOF. A similar trend was observed in the Paal–Knorr reaction, which similarly relies on the presence of *Lewis* acid sites. As expected, the catalytic activity of the OH-ip functionalized defective Ru-MOF samples were found to be superior to the unfunctionalized parent Ru-MOF. Another compelling example was performed by Llabrés and co-workers.<sup>[53]</sup> In their work, NH<sub>2</sub>-UiO-66/UiO-66 (UiO-66 with 2-amino-1,4-benzenedicarboxylate as linker) were used as solid acids in the esterification reaction of levulinic acid, whereby the number of missing linker defects inside UiO-66-NH<sub>2</sub> were estimated by using TGA. It was found that the rate constant correlates with the linker deficiency of the investigated systems (see **Figure 7**), demonstrating the strong impact of defects on the catalytic performance.

Furthermore, Dissegna et al. investigated the role of defects in the acid-catalyzed cyanosilylation of benzaldehyde.<sup>[19]</sup> In fact, controlling the degree of modulation of UiO-66 with AA and TFA enables the precise control of possible missing linker

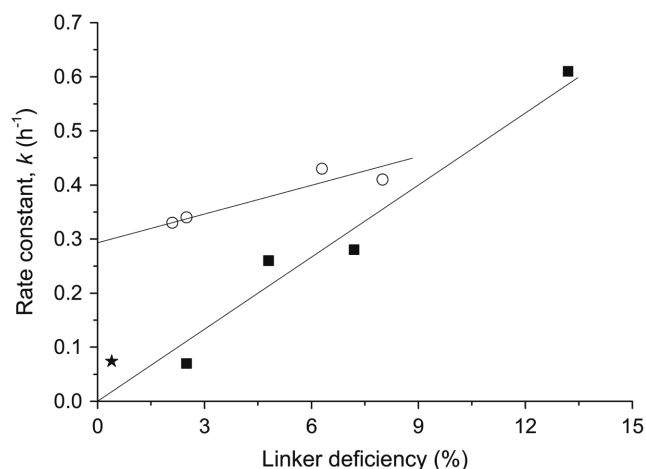


**Figure 7.** Dependency of the rate constant ( $k$ ) on the linker deficiency of the catalyst (pseudofirst order). Open symbols refer to UiO-66-NH<sub>2</sub> and closed ones to UiO-66, respectively. Reproduced with permission.<sup>[53]</sup> Copyright 2015, Elsevier.

defects, bearing additional  $-\text{OH}$  groups at the  $\text{Zr}_6$  nodes of the framework. Therefore, the  $\text{Zr}_6$  nodes are more accessible for given substrates and it is likely that the increased surface area of the defect engineered UiO-66 further helps to overcome diffusion limitations. The TFA-modulated UiO-66 sample was found to be significantly more active than the UiO-66 reference sample. Modulator-dependent defect engineering can also be used as a tool for pore design in order to facilitate diffusion and to incorporate different catalytically active species. Cai and Jiang reported on the fabrication of hierarchical UiO-66 containing mesopores using acetic/octanic/dodecanic acid as modulators.<sup>[54]</sup> The pore diameter in the obtained defective UiO-66 systems was systematically tuned via altering the length and concentration of the modulator, resulting in smaller or bigger mesopores within microporous UiO-66. The defect-induced formation of mesopores allows for the incorporation of larger catalytically active species like polyoxometallates, which then can be used in the catalytic methanolysis of styrene oxide. Notably,

hierarchical UiO-66 exhibits full conversion after 20 min, while reference UiO-66 shows no activity due to the absence of micropores.

### 3.2. Gas Adsorption

Due to their large porosity paired with the opportunity to chemically functionalize microchannels, MOFs are considered as promising gas adsorbers. During the past few years, it has been more and more recognized that the intrinsic adsorption properties can be tuned due to the introduction of new functional groups that can impact the interaction with different adsorbents such as  $\text{H}_2$ ,  $\text{CO}_2$ , and  $\text{CH}_4$ . Similarly, defects with their ability to alter the chemical functionalization of pores have been recognized to play a key role in adsorption processes.

In 2016 Szilágyi et al. reported on enhanced methane adsorption properties of postsynthetically treated MIL-101(Cr) by 33% compared to the pristine MOF.<sup>[55]</sup> In their work, they introduced  $\text{NH}_2\text{-BDC}^{2-}$  ( $\text{BDC}^{2-} = 1,4\text{-dicarboxylate}$ ) via SALE and were able to exchange up to 20% of the original  $\text{BDC}^{2-}$  linkers. However, the dramatic increase in  $\text{CH}_4$  uptake could not be explained by the introduction of new adsorption sites by the amino-functionalized linkers. The authors conclude that structural lattice point defects (see **Figure 8**) such as dangling linkers and missing linkers (linker vacancy) play an important role in the way that these defects open the pore windows of the MIL-101 superclusters, so the voids become more accessible for  $\text{CH}_4$ .

To exclude that only additional  $\text{NH}_2\text{-BDC}$  contributes to the increase in uptake, fully substituted  $\text{NH}_2\text{-MIL-101}$  was used as a reference system that shows a slightly reduced uptake. This is a remarkable example demonstrating that small changes, such as structural point defects, can in fact have a large impact on the properties of the overall framework. Another example that concerns with framework modification for  $\text{CO}_2$  adsorption was reported by Behrens et al.<sup>[56]</sup> In their study, they compared conventional electrical (CE) heating with microwave-assisted synthesis and studied the role of defects on the adsorption

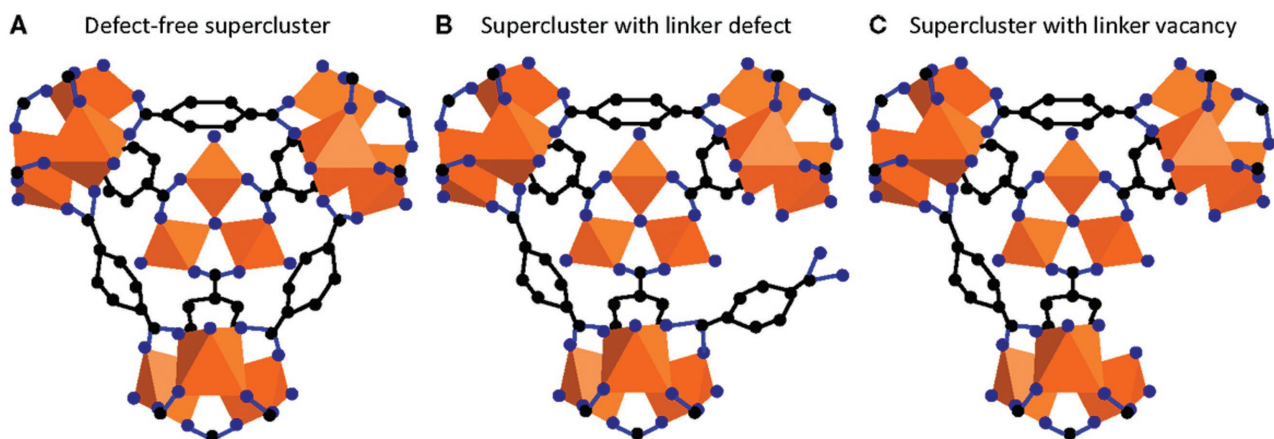


**Figure 8.** MIL-101 supercluster A) defect-free, B) with dangling linker, and C) with linker vacancy. The orange polyhedra represent the cationic units, whereas C and O atoms are depicted in black and blue, respectively. Reproduced under the terms of the CC-BY License.<sup>[55]</sup> Copyright 2016, P. Á. Szilágyi, P. Serra-Crespo, J. Gascon, H. Geerlings, B. Dam, Frontiers.



properties of differently functionalized imidazolate framework potsdam (IFPs). As already introduced, the formation of defects strongly depends on the applied synthesis conditions, whereby it is widely accepted that standard CE methods with long reaction times (usually days) allow for the growth of large crystals with a low defect density. The same group also applied microwave-assisted conditions, which lead to shorter reaction times (30–60 min) and samples with higher defect densities. To study the influence of these integrated lattice defects, the CE- and MV-synthesized IFPs were tested in CO<sub>2</sub> physisorption experiments. The authors found that the MV-synthesized IFPs outperform the conventionally synthesized IFPs, indicating the impact of defects on the adsorption properties.

Another important aspect in this context is the adsorption and capture of hazardous gases using porous materials. For instance, Rodriguez-Albelo et al. reported on the selective adsorption of sulfur dioxide using [Ni<sub>8</sub>(OH)<sub>4</sub>(H<sub>2</sub>O)<sub>2</sub>(BDP\_X)<sub>6</sub>] (H<sub>2</sub>BDP\_X = 1,4-bis(pyrazol-4-yl)benzene-4-X with X = –H (1), –OH (2), –NH<sub>2</sub> (3)) frameworks.<sup>[57]</sup> Defects were postsynthetically introduced via etching the respective MOFs with KOH solution, whereby certain amounts of linkers were replaced by –OH groups. The created missing linker defects and the incorporation of extraframework K<sup>+</sup> cations in turn increase the surface areas (those samples are abbreviated as 1,2,3@KOH). In a second PST step, K<sup>+</sup> was exchanged by Ba<sup>2+</sup> that is considered to have a positive effect on the SO<sub>2</sub> binding (abbreviated as 1,2,3@Ba(OH)<sub>2</sub>). The measured adsorption capacities at 303 K and at a low SO<sub>2</sub> partial pressure of 0.025 bar exhibited by the PST-treated nickel pyrazolate frameworks are relatively high, ranging from 2 mmol g<sup>–1</sup> for 1@Ba(OH)<sub>2</sub> to 5.6 mmol g<sup>–1</sup> for 3@Ba(OH)<sub>2</sub>. The affinity for SO<sub>2</sub> adsorption was found to be highest for the Ba<sup>2+</sup>-exchanged samples, followed by the KOH-treated samples and lowest by the parent samples, underlining the beneficial effects of KOH and the additional Ba(OH)<sub>2</sub> treatments on the adsorption of SO<sub>2</sub>. Interestingly, the isosteric heat of adsorption and Gibbs free energy values for SO<sub>2</sub> increase by ≈10–14 and 2–4 kJ mol<sup>–1</sup>, in the defective solids, suggesting the presence of strong interactions between adsorbed SO<sub>2</sub> molecules and the PST porous frameworks along the series 1@KOH–3@KOH, 1@Ba(OH)<sub>2</sub>–3@Ba(OH)<sub>2</sub>. Missing linker and cluster defects often cause damage within the structure of the framework and are associated with decreased chemical, thermal, and mechanical stability. Therefore, the framework must provide tolerance to such defects in order to maintain its stability. An interesting case facing this problem was reported by Lee et al. (see **Figure 9**).<sup>[34]</sup> The authors report on MUF-32 (Massey University Framework), which is built from Zn paddle wheel (PW) units as SBU, 4,4',4''-nitrotrisenbenzoate (ntb) as the tritopic organic linker and two neutral N-donor ligands 1,4-diazabicyclo[2.2.2]octane (dabco) and 4,4'-bipyridine (bipy), spanning a 3D net in the *itd* topology. This net can be interpreted as an *pto* net, which is constructed from Zn PW's nodes and ntb struts, forming a [Zn<sub>2</sub>(ntb)<sub>4/3</sub>] sublattice. Thus, the dabco and bipy ligands act as decorative ligands that can be

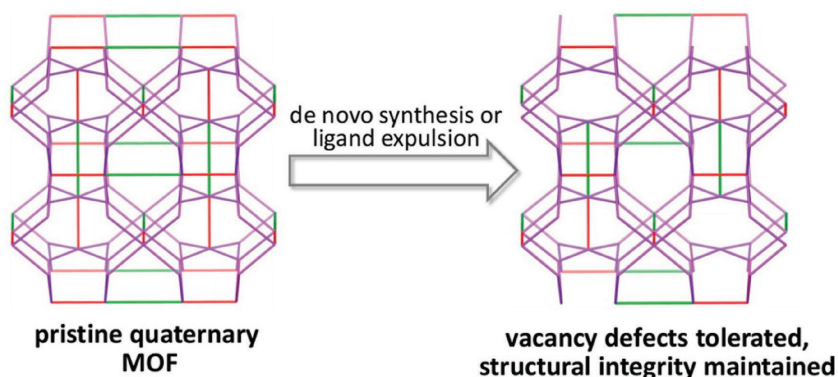


**Figure 9.** Formation of vacancy defects in MUF-32, whereby the structural *pto* sublattice is preserved. Reproduced with permission.<sup>[34]</sup> Copyright 2016, American Chemical Society.

removed without altering the structural integrity of the sublattice. Subsequently, the framework is highly tolerant to bipy or dabco vacancies (vacancy level up to 80%), which were introduced by varying the feeding ratios or PST methods such as soaking in DMF and thermal treatment.

Furthermore, those defects were successfully correlated with CO<sub>2</sub> adsorption, whereby systematic defect engineering in the de novo synthesis using substoichiometric levels of bipy produces MUF-32 samples with intrinsic bipy vacancies. Samples with higher bipy vacancies show higher CO<sub>2</sub> uptake in comparison to pristine MUF-32, indicating that defects improve the adsorption properties. The authors addressed these beneficial impacts on the different role of dabco. Due to the bipy vacancies, dabco binds on the axial position of the Zn PW in a monodentate fashion and acts as an N-donor, which can interact with CO<sub>2</sub>.

### 3.3. Decontamination

The chemical tunability of MOFs together with their porosity renders application of these materials in the areas of decontamination and detoxification, e.g., the adsorption of pollutants or chemical warfare agents (CWAs).<sup>[58–60]</sup> Different strategies for increased CWA detoxification have been investigated by Hupp and co-workers in the last few years. For instance, metal substitution (cerium-based UiO-66), MOF/polymer composites, enzyme immobilization, or detoxification via selective photooxidation have been developed in this context.<sup>[61–64]</sup> The utilization of photocatalysis or enzyme encapsulation is a nice proof-of-concept approach for CWA detoxification; however, there seem to be many practical challenges that need to be overcome in the future, e.g., enzyme preparation and isolation or a photocatalysis within gas masks is difficult to achieve. In the study by Plonka et al., capture and decomposition of dimethyl methylphosphonate (DMMP), a Sarin simulant, by defective Zr-based MOFs, were investigated.<sup>[59]</sup> In particular, they have used UiO-66, UiO-67, MOF-808, and NU-1000 to study the capture and hydrolysis of DMMP vapor through a stream of air or helium. By applying several analytics such as PXRD, DRIFTS (diffuse reflectance infrared Fourier transform spectroscopy), and EXAFS, they unambiguously assigned DMMP adsorption

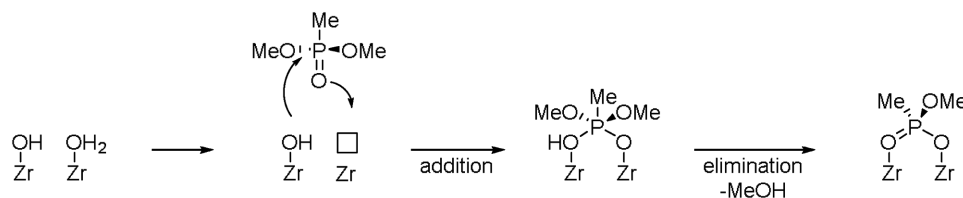


**Figure 10.** Schematic representation of DMMP degradation mechanism assumed in ref. [59].

occurring at CUS of the activated samples. Additionally, the authors studied the reaction mechanism of the decomposition of DMMP toward methyl methylphosphonate (MMPA) and methanol intensively. They correlate the activity with adjacent M–OH<sub>2</sub> and M–OH groups (see **Figure 10**), which are absent in defect-free UiO-66.<sup>[59]</sup> Thus, the role of defects for detoxification is crucial. It is envisioned that further synthesis optimization via defect engineering could be done for this purpose in the future. For instance, the modulator approach would lead to both higher adsorption capacities and faster hydrolysis, which might lead to a better performance in decontamination. Resulting MMPA shows a desorption energy from Zr centers of >100 kJ mol<sup>-1</sup>, leading to irreversible adsorption at ambient conditions.

López-Maya et al. have developed UiO-66-based composite materials, which are able to serve as self-detoxifying filters for CWAs.<sup>[65]</sup> By using the PST approach they intentionally induced missing linker defects and also additional acidic and basic sites in UiO-66 to improve the phosphotriesterase activity for capture and degradation of CWA simulants such as diisopropylfluorophosphate, dimethyl methylphosphonate, 2-chloroethylsulfide, and diethylsulfide. Defective UiO-66 samples in which defects were incorporated by the use of AA (UiO-66@AA) and KHSO<sub>4</sub> (UiO-66@SO<sub>4</sub>H) exhibit only slow CWA degradation kinetics paired with incomplete conversions due to product degradation and subsequent catalyst poisoning. In contrast, LiO<sup>t</sup>Bu-induced basic sites in UiO-66@LiO<sup>t</sup>Bu showed both full conversions and high activity in the degradation of all tested CWA simulants. It is important to mention here that UiO-66@LiO<sup>t</sup>Bu not only outperforms other MOF-based composite materials, but also some classical materials used for CWA decontamination such as activated carbon or porous metal oxides like ZrO<sub>2</sub>. Furthermore, lower sensitivity toward catalyst poisoning by degradation products or by additionally added methylphosphonic acid was observed with UiO-66@LiO<sup>t</sup>Bu. In order to further enhance applicability of UiO-66@LiO<sup>t</sup>Bu, it was integrated into silk fibrion fabrics as biocompatible, resistant, and lightweight textiles. By doing so, self-detoxifying and air permeable properties of both compounds were combined in one composite that showed the best performance in CWA simulant detoxification among all materials in their work.<sup>[65]</sup> While some studies<sup>[61,63,64]</sup> only tested liquid phase detoxification, the fiber/MOF composite<sup>[65]</sup> produced by López-Maya et al. was also applied under gas phase conditions.

Organoarsenic compounds, mostly phenyl arsenic acid derivatives, e.g., roxarsone (ROX), are used as feed additives but can be degraded into more toxic inorganic arsenic compounds that have already been found in meat and drinking water.<sup>[66]</sup> To date, there is no effective therapeutic treatment for arsenic poisoning. To date, there is no effective therapeutic treatment for

arsenic poisoning, and hence there is considerable interest in new decontamination procedures. B. Li et al. have used defect engineering in MOFs to obtain UiO-66 samples that show an increased adsorption behavior for ROX in aqueous solution.<sup>[60]</sup> They have used benzoic acid as modulator for the synthesis of defective (Zr) UiO-66. As expected, they observed an increase in BET surface from 600 m<sup>2</sup> g<sup>-1</sup> (“defect-free” sample) to 1568 m<sup>2</sup> g<sup>-1</sup> (20% modulator content related to BDC). Subsequently, the authors investigated important process parameters such as contact time, adsorbate concentration, pH as well as adsorption capacities. A formation of reactive Zr-OH groups as a result of missing linker defects mostly contributes to ROX adsorption and thus peaks in the 20% modulator sample. These additional binding sites lead to capacities up to 730 mg g<sup>-1</sup>. The reduced adsorption equilibrium times, 30 min compared to 240 min for “defect-free” UiO-66, were related to the presence of mesopores. A pH value of 4 turned out to be superior to more basic conditions regarding the ROX adsorption capacity. The authors explained this trend with an increasing electrostatic repulsion between negatively charged adsorbent and the ROX anions at higher pH-values. A negative influence of electrolytes such as common salts on binding affinities was also investigated and could be excluded. Reusability was proven and includes an almost complete release of ROX in diluted hydrochloric acid after each cycle.

### 3.4. Dye Uptake and Degradation

Organic dyes are widely used in different industries like paintings, leather, furniture, textile, and paper production. Depending on the process, certain dyes can cause environmental problems due to their low biodegradability.<sup>[67,68]</sup> Hence, efficient dye uptake as well as degradation methods is required. There are several publications in the field of (defective) MOFs that deal with this topic. For instance, Cai and Jiang et al. have not only used their hierarchically porous (HP; micro and mesoporous) (HP)-MOFs (UiO-66, UiO-66-NH<sub>2</sub>, UiO-66-NO<sub>2</sub>, UiO-67, MIL-53, MIL-53-NH<sub>2</sub>, DUT-5 (Dresden University of Technology)) and MOF-808 in catalytic reactions, as mentioned in the catalysis part, but also for dye uptake of coomassie brilliant blue R250. In contrast to pristine “defect-free” UiO-66 (only micropores available), the color of the dye solution faded while the white powder turned blue during dye uptake.<sup>[54]</sup>

Fan and co-workers have conducted a defect engineering study following the mixed-linker approach and explored the use of rhodamine B (RhB) degradation with metalloligands. More precisely, carboxy substituted tris(bipyridine) iridium complexes were used as metalloligands (see **Figure 11**, left panel). Both parent (ZnIr-MOF, for crystal structure see **Figure 11**, middle

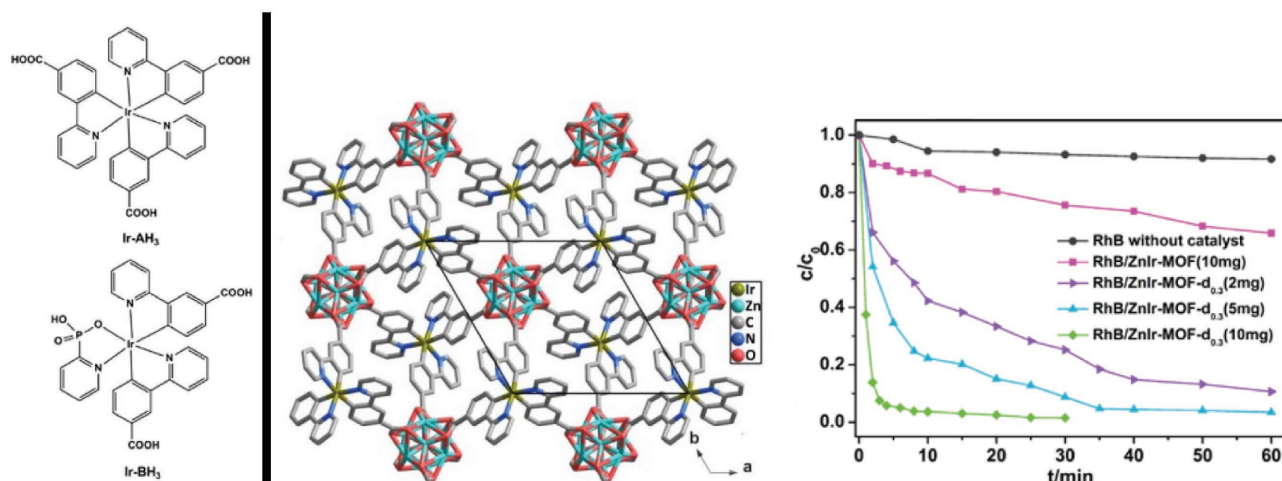


**Figure 11.** Left panel: Parental Ir-AH<sub>3</sub> and defective Ir-BH<sub>3</sub> linker applied in the work of Fan et al. Middle panel: 2D structure representation of ZnIr-MOF. Right panel: Comparison of materials in RhB degradation. Reproduced with permission.<sup>[68]</sup> Copyright 2017, John Wiley & Sons.

panel) and defective materials (ZnIr-MOF-d<sub>0.1-0.9</sub> depending on the amount of defective linker) were characterized intensively including a series of adsorption studies, diffuse reflectance UV-vis spectroscopy, and fluorescence measurements. Interestingly, the defective material ZnIr-MOF-d<sub>0.3</sub> exhibits a much larger emission lifetime (2.53 μs) than parental ZnIr-MOF (1.85 μs) although both isolated linkers Ir-AH<sub>3</sub> and Ir-BH<sub>3</sub> are quite similar (1.76 and 1.66 μs respectively). The observed prolonged emission lifetimes and semiconducting properties (2.4 eV band gap) are important requirements for photocatalysis. Consequently, they applied the material in the degradation of RhB. It turned out that defective ZnIr-MOF-d<sub>0.3</sub> is significantly more active than the parent MOF, cf. kinetic curves in Figure 11 (right graph). The higher activity can mainly be attributed to increased hydrophilicity, micro- and mesoporosity and light harvesting. By now, this is the only report of defect engineering of an Ir-based MOF and its dramatically increased performance in dye degradation is a good example of the potential of defective MOFs.<sup>[68]</sup>

### 3.5. Hydrophobicity

One of the most significant MOF drawbacks is their affinity toward water that limits their application in industry. Particularly, zinc/carboxylate-based MOFs are extremely sensitive to moisture due to the nature of the bonding between zinc atoms and carboxylate ligands. Some MOF materials, such as MIL-101-Cr, MIL-100-Fe, UiO-66, ZIF-8, and NU-1000, are resistant to moisture but their CO<sub>2</sub> adsorption capacities are not satisfactory. For this reason, much effort has been put on improving water stability of MOFs thereby overcoming this drawback and, at the same time, improve CO<sub>2</sub> adsorption capacities through different postsynthetic treatments such as SALE, linker functionalization with hydrophobic groups (i.e., fluorinated groups), or simply via physical adsorption as shown by Fernandez et al.<sup>[69]</sup> In their work, MIL-101 (Cr) was chosen as a starting material due to its reasonably good CO<sub>2</sub> capture properties and its resistance to water only for short period of time. The authors

physically adsorbed amphiphilic moieties on the external MOF surface. In such a scenario, the polar side coordinates the open metal center present on the MOF surface while the hydrophobic chain points outside, protecting the MOF against moisture without compromising its CO<sub>2</sub> capture ability.

In another recent work, Deria et al. introduced perfluorinated carboxylic acids in NU-1000 via SALI. These hydrophobic groups strongly coordinate the CUS presents in NU-1000 improving its CO<sub>2</sub> capture ability due to the interaction between the CO<sub>2</sub> quadruple and the dipole moment of the C-F bonds.<sup>[35]</sup> Moreover, the fluorinated modified NU-1000 was used for C-H arylations of indoles in a water medium as shown by Huang et al. (see Figure 12).<sup>[70]</sup> The authors used this MOF as support for Pd NPs, which offers particular environmental and sustainable advantages since water is the most inexpensive and environmentally friendly solvent (see Figure 12). Therefore, the chemical manipulation of CUSs is a simple and effective way to improve the catalyst performance not only in the aspects of the chemical stability (water stability), but also in their performance in gas adsorption and catalysis.

### 3.6. Charge Transport in MOFs

Another exciting research field in the context of this review depicts the realization of charge transport in MOFs. This is a desired property for many applications such as photo- and electrocatalysis, energy harvesting (solar cells) and energy production (fuel cells) or electronic devices and semiconductors, among others. Despite the large list of potential fields of applications, the number of research groups focusing on electrically conductive MOFs is yet limited. Inherently, the type of chemical bonding in MOFs, i.e., the coordination bond chemistry, turns MOFs into electrical insulators. However, by judiciously designing frameworks including the aspect of intentional doping and defects, it is in fact possible to introduce charge transport pathways, e.g., through close π-π interactions or the incorporation of delocalized radicals.<sup>[71]</sup> Similarly, the implementation of high ionic conductivity would be interesting in the fields of batteries or solid-state







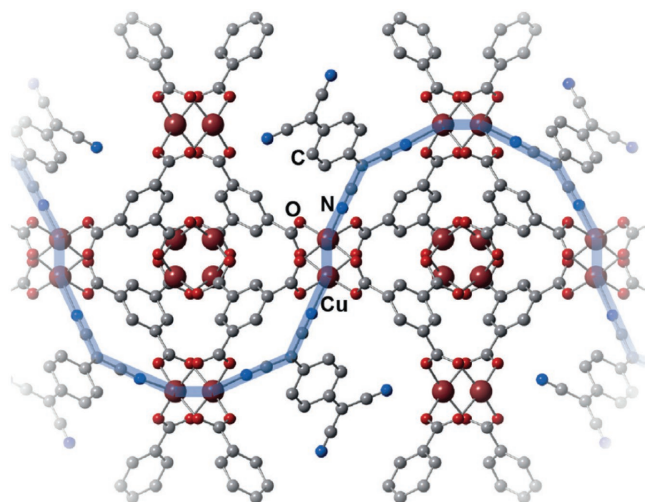


**Figure 14.** Predicted TCNQ integration in HKUST-1 and proposed covalent charge-transport pathway (through-bond) highlighted in blue. Reproduced with permission.<sup>[71]</sup> Copyright 2016, John Wiley & Sons.

and thin films have been loaded with TCNQ and intensively studied by Allendorf and others during the last few years.<sup>[87–91]</sup> In fact, loading of HKUST-1 with one TCNQ molecule per pore increases the electronic conductivity from  $10^{-8}$  to  $0.07 \text{ S cm}^{-1}$  with a resulting activation energy of  $0.041 \text{ eV}$ .<sup>[88]</sup> Holes are expected to be the responsible charge carriers based on a positive Seebeck coefficient.<sup>[87]</sup> An assumed transport pathway is depicted in **Figure 14**.<sup>[71]</sup> Note that this scheme is idealized. Within our definition of defects and disorder it should be noted that the existence of a highly ordered and stoichiometric loading of TCNQ leading to a second coordination network within the parent framework is strictly speaking not supported by rigorous experimental evidence. Rather it seems likely that this TCNQ adsorbate structure is very rich in defects. The elucidation of the defect structure and chemistry related to the electrical conductivity of TCNQ loaded HKUST-1 deserves attention.

A drawback of the loading approach is a significant reduction of accessible pore volume due to guest incorporation. For instance, the BET surface area of more than  $1800 \text{ m}^2 \text{ g}^{-1}$  in pristine HKUST-1 is dramatically reduced to  $214 \pm 0.5 \text{ m}^2 \text{ g}^{-1}$  after TCNQ loading.<sup>[88]</sup> Furthermore, the limitation to one TCNQ molecule per pore seems to also limit the maximal conductivity value since only 50% of the overall CUS number can be occupied and interconnected. Nevertheless, MOF tunability regarding conductivity is easily achieved with doping and loading strategies. We here like to refer to a conceptual article on guest@MOF systems, published by Allendorf and our group.<sup>[92]</sup> Additionally, there are other illuminating articles that specifically address the use of MOFs in energy-related applications,<sup>[93]</sup> for electroacoustic<sup>[91]</sup> or resistive sensing devices.<sup>[94]</sup> Besides that, a roadmap for the integration of MOFs into electronic devices and chemical sensors was already proposed in 2011 and updated in 2017.<sup>[72,95]</sup> Although there has been a huge growth in the field of electrical conductivity in MOFs (irrespective of the chosen approach) compared to gas sorption and catalysis, the field is still in its youth and is expected to grow further in the near future. We would like to emphasize at this point that

understanding defects and disorder in such systems will be of paramount importance for achieving quantitative structure–function relationships and matching theoretical expectations with experimental data (see the next paragraph).

### 3.6.2. Ionic Conductivity

Ionic conductivity (IC) describes charge transfer through transport of ionic species in a material. As an important subset of IC, proton conductivity (PC) plays a key role in processes as diverse as the photosynthesis in green plants and more recently the production of electricity in fuel cells.<sup>[96]</sup> Various compounds such as Nafion®, sulfates, selenates, phosphates, and many more have been discovered in the past decades. Due to the high chemical tunability and their porous structure it is no surprise that MOFs are also being examined in the context of ionic conduction and in particular as proton conductors.<sup>[97,98]</sup> Generally speaking, there are different approaches how to establish or improve PC in MOFs. The most obvious one is the introduction of counterions such as  $\text{NH}_4^+$ ,  $\text{H}_3\text{O}^+$ , and  $\text{HSO}_4^-$  into the framework pores. In this case, the introduced groups are physisorbed species with mainly ionic interactions to the framework.<sup>[99]</sup> Other approaches focus on inherently acidic frameworks, either by self-assembly of by using the corresponding functionalized ligands or by postsynthetic modifications of a parent MOF.<sup>[99]</sup> In such approaches, the acidic groups, such as carboxylic, phosphonic, or sulfonic acids, are covalently bound within the framework as nonstructural ligands, either attached to the organic linker or to the secondary building units (SBUs).<sup>[100,101]</sup> However, it was shown that the number of newly generated acidic protons is not the only factor for the enhancement of PC in MOFs. In a recent work, Kitagawa and co-workers reported on the combination of increasing Lewis acidic sites that provide a mobile proton with coordinated water as well as improving the mobility of the protons using defect engineering in order to tune the porosity in UiO-66.<sup>[102]</sup> For this purpose, defects were systematically introduced via understoichiometric use of terephthalate linker compared to Zr and the use of monoacids such as acetic and stearic acid. The PC of the resulting materials was tested using AC impedance analysis, whereby an increase from 5 to 23% in ligand defects causes a remarkable increase in PC by almost two orders of magnitude at  $65 \text{ }^\circ\text{C}$  (from  $1.30 \times 10^{-5}$  to  $1.01 \times 10^{-3} \text{ S cm}^{-1}$ ).

Furthermore, the authors report on the surprisingly high PC in the sample where stearic acid was used as a template molecule, even though it was not incorporated into the framework, and which contains less defects than the previous samples using acetate. These on the first sight contradicting findings are explained to the beneficial effect of increased surface area, implicating interparticular transport of ions. Moreover, stearic acid treated MOF samples are found to be more hydrophilic, providing higher total water uptake. Another example by the same authors tackles the multifaceted consequences of defects in sulfonated UiO-66, which can appear to be negative in some cases.<sup>[103]</sup> Hereby, a derivative of UiO-66 was synthesized, carrying sulfonate groups at the terephthalate linkers which provide a high concentration of charge carriers, namely acidic protons (see **Figure 15**). Careful structural analysis reveals a quite

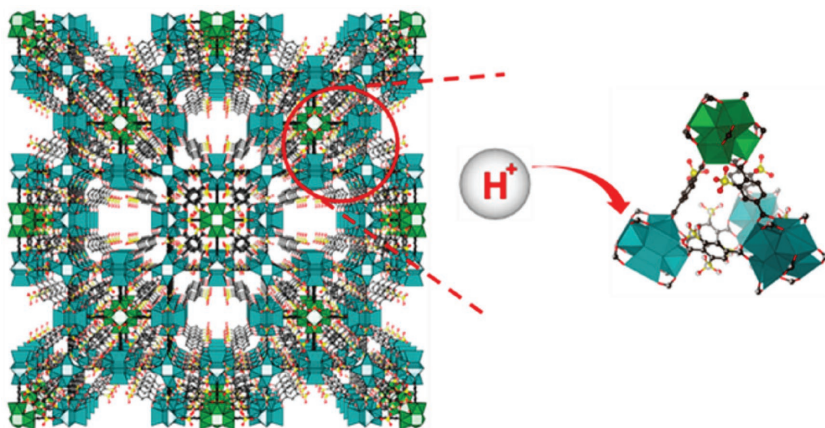


**Figure 15.** Proton conductivity in sulfonated UiO-66. Reproduced with permission.<sup>[103]</sup> Copyright 2015, American Chemical Society.

complicated defective structure, displaying a large number of partially occupied ligands and zirconium centers within the lattice. A roughly double sized unit cell compared to regular UiO-66 was observed, which was attributed to “vacant  $Zr_6$ -cluster sites.” This results in the presence of 12-fold as well as 9-fold connected  $Zr_6$  clusters. Moreover, it was found that the experimentally observed Zr/S ratio is higher than the theoretical one (1.43 vs 1.3), leading to a discrepancy that is attributed to partially occupied atomic positions at the 9-connected  $Zr_6$  cluster. These provide a structure with high amount of linker vacancies and a continuum of different pore sizes. Despite the relatively high density of acidic sulfonic acid groups, the conductivity is found to be more than one order of magnitude smaller than in many other MOF systems under similar conditions. Supporting DFT calculations reveal that the defects, namely the Zr–OH defect site, provides moderate basicity ( $pK_a$  of 13.3) and is believed to be a trapping agent for the protons, reducing the total amount of charge carriers. As a next step, the authors successfully demonstrate that these sites can be saturated with strong acids. The acid-treated samples show a significantly improved PC with a maximum of  $5.62 \times 10^{-3}$  and  $3.46 \times 10^{-3} \text{ S cm}^{-1}$  at 95% RH, respectively, with activation energies of 0.24 and 0.25 eV at 95% RH. This work highlights the importance of careful analysis of the exact nature of the present defect structure. Only if one can understand the defects and transport mechanism, it is possible to find solutions how to overcome these specific defect-derived challenges, providing materials with improved PC. Similarly, the conductivity of hydroxide-ion using MOFs is of interest but relatively unexplored.<sup>[104]</sup> Montoro et al. investigated the role of defects on hydroxide-ion conductivity using  $[Ni_8(OH)_4(H_2O)_2(BDP\_X)_6]$  ( $H_2BDP\_X = 1,4\text{-bis(pyrazol-4-yl)benzene-4-X}$  with X = H (1), OH (2),  $NH_2$  (3)) MOF as a test system in order to fine tune the conducting properties utilizing a postsynthetic treatment with KOH–EtOH solution.<sup>[105]</sup> Consequently, missing linker defects were introduced by partial linker dissolution enhancing the overall porosity, which in turn is beneficial for the mobility of charge carriers. Another effect was the enhanced basicity and hydrophilicity of the framework due to deprotonation of water, which was bound to the Ni nodes, and the incorporation of extraframework  $K^+$  cations. Hence, an increase of conductivity three to four orders of magnitude compared to

the pristine materials has been observed ( $1.16 \times 10^{-2} \text{ S cm}^{-1}$  ( $E_a = 0.20 \text{ eV}$ )) at a relative humidity of 100%. Notably, when measuring IC, it is important to distinguish between inter- and intraparticle ionic conductivity. One way is testing IC/PC by using single-crystal conductivity measurements in order to clarify whether protons are transported through the lattice and/or micropores or through interparticle phases.<sup>[106]</sup> For instance, Tominaka and Cheetham critically discussed a range of measurements of different MOFs and zeolites, proposing that hydrated interparticle phases might make a considerable contribution to proton conduction in many MOFs when measurements are made on pellets.<sup>[106]</sup> In order to better understand the conducting pathways in MOFs, measurements on single crystals are more suitable to

distinguish between intrinsic/extrinsic conductivity. However, it is not always possible to grow single crystals of MOFs which are suitable for the measurement, which might challenge future studies.

#### 4. Computational Modeling of Defects in MOFs

In this section, some key messages are compiled which were extracted from the still quite few focused studies on computational modeling of defective MOFs which appeared since 2015 (Table 1).<sup>[23,109,111,116,121,127,129,132,136,140,142]</sup> The systems of choice were mainly UiO-66 and its isorecticular expanded versions.<sup>[109,116,129,136]</sup> Some related work was also done on ZIF-8,<sup>[140]</sup> IRMOF-1,<sup>[116]</sup> and HKUST-1.<sup>[111]</sup> One important common issue was the question how concentration and spatial arrangement (correlation) of missing linker defects are interdependent and may affect at the same time both the gas sorption properties and the mechanical stability. The systematic study by Thornton et al. on various defect scenarios included modulator dependence, defect concentration, clustering, and ordering of defects.<sup>[127]</sup> Generally, mechanical stability is lowered with increasing defect level. Turning this issue the other way around, structural flexibility and stimuli responsiveness can be implemented in otherwise rigid MOFs by defects. Figure 16 shows the simulated  $CO_2$  uptake at low (1 bar) and at high (30 bar) pressures and Young's modulus as functions of the number of missing linker defects.<sup>[127]</sup> Importantly, clustering and ordering of defects at a short-range length scale as it is the case for the high symmetry *re*o type of missing linker/node defective UiO-66 “offers a more stable structure coupled with an increase in uptake at high pressures.”<sup>[14]</sup>

Van Speybroeck and co-workers provided a thermodynamic characterization of the high-pressure behavior of UiO-66 as a function of missing linker defects and linker expansion in the absence of guests.<sup>[23]</sup> On the atomistic level, the phenomenon is reflected in a sudden drop in the number of symmetry operators for the crystallographic unit cell because of the disordered displacement of the organic linkers with respect to the inorganic

**Table 1.** The most relevant publications on defective MOFs in 2015–2017.

Compound	Defect engineering	Characterization	Function/property	Ref.
Ni-based MOF	Etching/Ion-exchange	BET, XRD, TGA	SO <sub>2</sub> adsorption	[57]
Ni-based MOF	PST with KOH	Elemental analysis (EA), BET, water adsorption	Ion conductivity, hydrophilicity	[105]
CPO-27-M	Substitution of DOBDC with BDC-OH	PXRD, BET, TGA	–	[107]
Cu[Ni(pdt)]	Iodine doping approach	Conductivity, PXRD, BET, DR-UV/VIS, CV	Electronic conductivity	[85]
DUT-5	Mesopores tuned by different modulator and linker insufficiency	PXRD, BET, TGA	Dye and particle uptake and catalysis	[54]
FDM-21	Defects created by defective ligand	XRD, BET, TGA, NMR	Acetylene storage	[108]
Fe-based MOFs	Computational study	DFT calculation, BET, ICP	Ethane oxidation	[109]
Fe based MOF	Iodine doping approach	XRD, BET, VT magnetic susceptibility, TGA, EA, CV, UV-vis, EPR	Electronic conductivity	[86]
HIF-3	Microwave synthesis (fast crystal growth)	PALS	–	[45]
HKUST-1	Defect created by defective ligand	XANES, UHV-FTIR, XPS	Paal–Knorr reaction	[52]
HKUST-1	Change of synthesis parameters	XPS	–	[110]
HKUST-1 (Ru)	Solid solution	UHV-FTIR, etc.	–	[25]
HKUST-1	Loading approach (TCNQ)	Conductivity, PXRD, BET, DR-UV/VIS, EPR, Raman,	Electronic conductivity, thermoelectric devices	[87–91]
HKUST-1	Computational study	Coarse-grain force field calculations	Study on mechanical and structural stability	[111]
HKUST-1	Effects of synthetic conditions and activation procedure	–	Hexane, 1-hexene separation	[112]
HKUST-1	solid solution, mixed-linker approach	Standard, BET	Catalysis	[113]
HKUST-1	Mixed-linker approach	High-pressure gas adsorption properties studied (H <sub>2</sub> , CO <sub>2</sub> , CH <sub>4</sub> )	–	[114]
IFP-11 to IFP-13	Microwave synthesis (fast crystal growth)	CO <sub>2</sub> adsorption, PXRD and DFT calculations	Improved CO <sub>2</sub> gas uptake	[56]
In-MIL-68	Modulation approach	SEM, XPS, photo luminescence	Mechanism of MOF formation	[115]
IRMOF-1	Defects' modeling and study of the influence on the properties	Simulated Ar isotherms	–	[116]
MIL-53	Mesopores tuned by different modulator and linker insufficiency	–	Dye and particle uptake and catalysis	[54]
MIL-101	PST, activation	BET	Knoevenagel condensation reaction	[117]
MIL-140	Investigation of amorphization of MOFs	SS- <sup>13</sup> C-NMR, PDF	–	[38]
MIL-101 (Cr)	SALE	DRIFTS	Gas storage	[55]
MIL-53 (Al)	PST (ball milling)	Acetylene adsorption, field emission SEM	Acetylene storage	[118]
MOF-74 (Mn)	Defects created by defective ligand	XRD, BET, TGA, NMR	–	[108]
MOF-808	Mesopores tuned by different modulator and linker insufficiency	–	Dye and particle uptake and catalysis	[54]
MOF-808	Modulation approach	Potentiometric acid–base titration	–	[47]
MOF-808	Modulation approach	Potentiometric acid–base titration	Styrene oxide ring-opening reaction	[48]
MUF-32	PST (high-temperature activation)	BET, XRD, NMR	CO <sub>2</sub> adsorption	[34]
NU-1000	Modulation approach	Potentiometric acid–base titration	–	[47]
NU-125	PST (SALE)	DRIFTS, XRD	Post-synthesis methylation	[33]
NU-125	Mixed-linker approach	High pressure gas adsorption (H <sub>2</sub> , CO <sub>2</sub> , CH <sub>4</sub> )	–	[114]
PCN-57	Modulation approach	Potentiometric acid–base titration	–	[48]
Sulfonated NUS-6	Modulation approach	Potentiometric acid–base titration	Dehydration of fructose	[119]
UHM-3	PST (thermal treatment) on SURMOFs	IR-RAS with CO, XPS, and CO <sub>2</sub> adsorption measurements	–	[120]

**Table 1.** Continued.

Compound	Defect engineering	Characterization	Function/property	Ref.
UiO-66	Computational study on defects	DFT	–	[121]
UiO-66	Modulation approach	Potentiometric acid–base titration	–	[48]
UiO-66	Modulation approach	XRD, BET, TGA	Mechanism of MOF formation	[115]
UiO-66	Microwave synthesis and modulation approach	Energy-dispersive spectroscopy	CO <sub>2</sub> and water adsorption	[122]
UiO-66	–	–	NH <sub>3</sub> adsorption	[123]
UiO-66	Modulation approach, metalated-ligand-exchange	–	CO <sub>2</sub> adsorption	[124]
UiO-66	PST Functionalization of defect with amino acids	NMR, BET, XRD	–	[125]
UiO-66	Modulation approach with fatty acids	Conductivity experiments	Proton conductivity	[102]
UiO-66	Tune of the already existing CUS sites	Extensive IR study, DFT calculation	–	[126]
UiO-66	Modulation approach	XRD, BET, TGA, NMR	–	[17]
UiO-66	Computational study	Simulated BET, Young modulus, CO <sub>2</sub> uptake	CO <sub>2</sub> gas adsorption	[127]
UiO-66	Computational study of CUS environment	SCXRD	–	[128]
UiO-66	Computational study of defective sites in UiO-66	Very detailed computational study	–	[129]
UiO-66	Defect created by defective sulfonated ligand	Conductivity experiments, DFT calculation	Proton conductivity	[103]
UiO-66	Theoretical study of defects effect on the UiO-66 physical properties	DFT, quick FF	–	[23]
UiO-66	Computational study	Simulated water, CO <sub>2</sub> adsorption isotherms, heat of adsorption	–	[130]
UiO-66	Modulation approach	Water adsorption measurements	Cyanosilylation of benzaldehyde	[19]
UiO-66	–	Study on MOF electronic structure	Possible photocatalysis	[131]
UiO-66	Computational study	PXRD reflexes, DFT calculation with supercell approach	–	[14]
UiO-66	Computational study	Atomistic force field, DFT	–	[132]
UiO-66	Modulation approach	PXRD BET, NMR	–	[39]
UiO-66(Hf)	Computational study	Defects' influence on negative thermal expansion	–	[133]
UiO-66	PST (ball milling)	SS- <sup>13</sup> C-NMR, PDF	–	[38]
UiO-66	Mesopores tuned by modulator choice and linker insufficiency	–	Dye and particle uptake and catalysis	[54]
UiO-66 and UiO-66-NH <sub>2</sub>	Modulation approach	XRD, BET, TGA	Esterification of levulinic acid	[53]
UiO-66 and UiO-67	Modulation approach	XRD, BET	Cyclisation of acetaldehyde	[134]
UiO-67 (hcp)	Ligand-deficient synthesis toward porous 2D materials	–	Catalysis	[135]
ZIF-8	Computational study	–	–	[136]
ZIF-8	Modulation approach	TGA, BET, IR	Gas separation	[137]
ZIF-8	Modulation approach	TGA, BET, SS-NMR	Gas separation	[138]
ZIF-8	Computational study	Theoretical study	–	[139]
ZIF-8/PIMs	Computational study	DFT calculation	–	[140]
Zr-fumarate	Modulation approach	In situ IR	–	[141]

CV: Cyclic Voltammetry; DFT: Density Functional Theory; EPR: Electron Paramagnetic Resonance; FDM: Fudan Material; FF: Force Field; ICP: Inductively Coupled Plasma; NUS: National university of Singapore; UHM: University of Hamburg Materials; RAS: Reflectance Anisotropy Spectroscopy; SCXRD: Single Crystal XRD; SS: Solid State; XPS: X-Ray photon Spectroscopy

nodes. For the defect-containing and/or expanded linker samples, a reduced mechanical stability is observed. Two regimes were identified. Around the equilibrium volume, a quasilinear

pressure-versus-volume dependence  $P(V)$  is retrieved, which indicates that the material satisfies Hook's law (**Figure 17**). Increasing missing linker defects reduces the average node



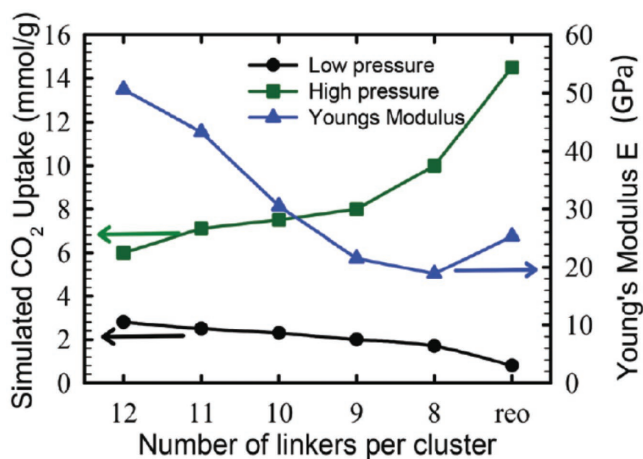


**Figure 16.** Simulated CO<sub>2</sub> uptake at different pressures and Young's modulus as a function of the average number of linkers per zirconium oxo cluster of UiO-66, which represents various scenarios of missing linker defects. Reproduced with permission.<sup>[127]</sup> Copyright 2016, Royal Chemical Society.

connectivity and the maximum of the  $P(V)$  function shifts to lower values and larger critical cell volumes. It turned out that this kind of correlation of defects is of paramount importance for the mechanical properties (Figure 18). *Type 3* defect refers to the removing of two linkers in such a way that 1D channels are created in the material. In this case, the mechanical stability remains exceptionally intact. In contrast, for the *type 5* defect, a relatively strong deterioration of the mechanical properties is observed (see insets in Figure 18). This phenomenon is due to the equal orientation of the two removed linkers on different planes which facilitate sliding along these crystallographic directions.

Gale and co-workers calculated the free energy of ligand removal in UiO-66, again for different defect scenarios including

solvation phenomena. Their results on mechanical properties match well with the above-highlighted results.<sup>[132]</sup> For a missing BDC, the lowest energy charge-capping mechanism involves CH<sub>3</sub>COO<sup>-</sup> or Cl<sup>-</sup>/H<sub>2</sub>O. The calculated free energy of defect formation in solution is remarkably low (e.g.,  $\approx 120$  kJ mol<sup>-1</sup> at 300 K for a single linker vacancy capped with acetate). Linker cluster formation following the removal and protonation may occur both in the framework but also between the removed species in the solvent. A strong binding energy of  $-75.3$  kJ mol<sup>-1</sup> between DMF and H<sub>2</sub>BDC was calculated, supporting the solvent-dependent mechanism of defect generation. The study also provided nice evidence for the possibility to identify (and quantify) the binding of modulators to the nodes by IR spectroscopic signatures. Sholl and co-workers investigated the kinetic feasibility of local defect formation of ZIF-8 with the perspective of the reactivity and long-term stability under working conditions that may involve exposure to water or acidic gases.<sup>[136]</sup> Linker vacancy, zinc vacancy, and dangling linker defects were considered formed upon protolytic cleavage of zinc-linker bonds. Typical charge compensation (capping) groups at adjacent Zr centers of the point defective ZIF-8 structure were OH<sup>-</sup>/H<sub>2</sub>O, CH<sub>3</sub>COO<sup>-</sup>/H<sub>2</sub>O, and OH<sup>-</sup>/HmIM (2-methylimidazole). Solvation effects were included. Most of the formation energies were found to be thermoneutral or even exothermic which point to the likeliness of defect formation under ambient conditions. These results suggest a possible mechanism for the so-called postsynthetic linker<sup>[31,143–145]</sup> and metal exchange processes in ZIFs and possibly beyond.<sup>[144,145]</sup> Such single crystal transformations could be driven by the transient formation of defects.

Sarkisov focused on the origin of correlated defects causing mesoporosity with IRMOF-1 as the case study.<sup>[116]</sup> In a first approach, linkers were randomly removed from the structure with increasing defect level (5%, 10%, and 20%). Starting by about 50% of defects, the calculated adsorption isotherms ( $A_r$ ) and the corresponding pore size distributions change drastically. At 73% of linkers removed, the isotherm corresponds to

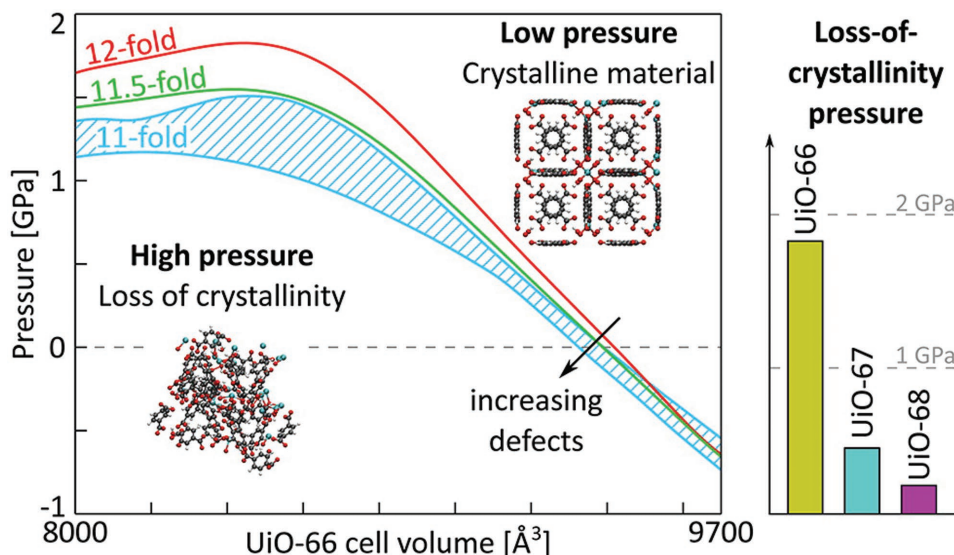


**Figure 17.** Mechanical stability and loss of crystallinity upon external pressure for UiO-66, 67, and 68 as a function of defect linkers and linker expansion. Generally, the loss-of-crystallinity pressure (maximum of the  $P(V)$  curve) drastically decreases with linker expansion and with reduction of the average connectivity of the nodes by missing linker defects. Reproduced with permission.<sup>[23]</sup> Copyright 2016, American Chemical Society.

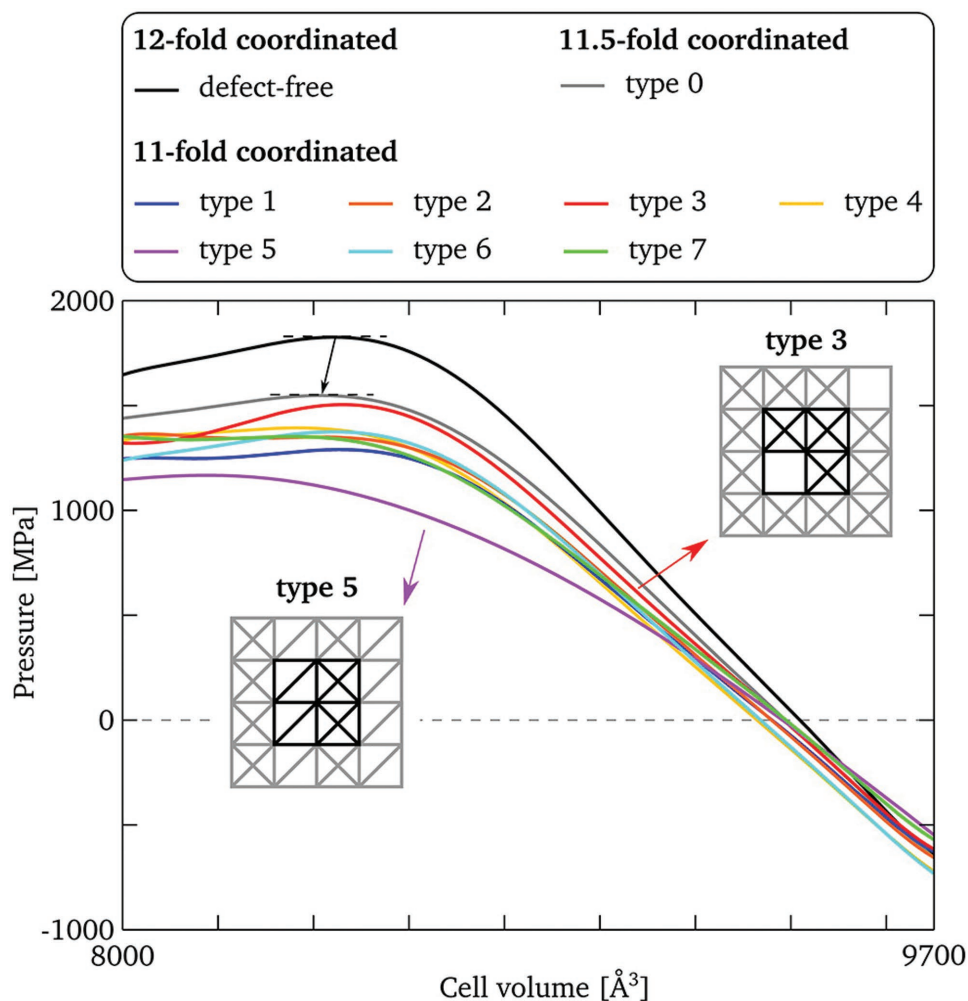


**Figure 18.** Internal pressure  $\langle P_i \rangle$  as a function of the constrained unit cell volume  $V$  for the defect-free UiO-66 and the different defect-containing materials, resulting from simulations at  $T = 300$  K, with indication of the initial decrease in loss-of-crystallinity pressure when introducing the first linker vacancy. Insets: Schematic depiction of defect structures *type 3* (right) and *type 5* (left). Reproduced with permission.<sup>[23]</sup> Copyright 2016, American Chemical Society.

an intermediate type 4 and 5 and featuring a hysteresis loop, which indicates mesopores (Figure 19). However note that such a scenario at very high levels of missing linkers has not been verified experimentally. In fact, the onset mesoporosity was observed at much lower defect linker concentrations. An alternative model is a local clustering of missing linker defects and the existence and random distribution of regions of mesoporosity within a uniform microporous (perfect) crystalline matrix. The authors considered a model of two unit cell wide sheets of IRMOF-1 crystals separated by a 20 Å gap (Figure 20). This model gave a better match with the experimental data.

Schmid and co-workers<sup>[111]</sup> performed an in-depth study on the mesopore formation based on the experimental work on defect engineered HKUST-1 by Fang et al.<sup>[148]</sup> They combined a maximally coarse-grained force field for HKUST-1<sup>[149]</sup> with a systematic scheme to regenerate the atomistic structure from a vertex-based representation.<sup>[150]</sup> In this way, they have been able to simulate various defect scenarios and investigated trends in mechanical stability, as well as changes in surface area and pore size distribution induced by spherical

mesopores carved into HKUST-1. As expected, the mesopores resulting from clustered missing node defects lead to a continuous reduction in the bulk modulus with an increasing degree of defects. However, for a constant relative mesopore void volume, a higher mechanical stability is observed in cases of larger cavities. In the case of smaller cavities, a slight increase of the gravimetric surface area was found. The authors finally state that “In the limiting case for large cavities, in which the surface effects become less and less important, the volumetric surface area decreases as expected, whereas the gravimetric surface area stays constant with increasing levels of defects. Consequently, variations in the measured surface areas in different samples are not necessarily due to pore collapse but to different amounts of incorporated mesoporous defects.” There are few other computational studies on defective MOFs dealing with various issues related to catalytic properties including water coordination and dehydration processes,<sup>[129]</sup> dynamic acidity associated with hydroxide capping groups,<sup>[121]</sup> and grafting of molecular (organometallic) catalysts at missing linker defect sites at the nodes.<sup>[151]</sup> These studies are quite

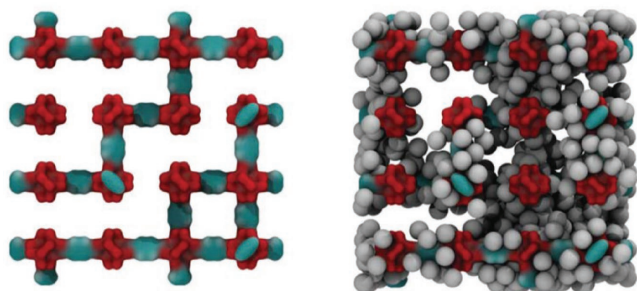


**Figure 19.** Left panel: Visualization of the defect IRMOF-1 model structure with 73% of linkers removed. Over the periodic boundary conditions, the structure still forms a continuous, self-supporting network. Right panel: The structure filled with argon molecules at 78 K, prior to the condensation step. Color scheme: Cyan for carbon, red for oxygen, and gray for argon. Reproduced with permission.<sup>[116]</sup> Copyright 2016, Royal Chemical Society.

enlightening and provide perspectives of how defect scenarios and reactive processes may be coupled.

## 5. Conclusion

After summarizing the recent progress of the field, it is apparent that the defect chemistry of MOFs contains a great deal of opportunities for creating and tuning application relevant properties and is further deepening our fundamental knowledge of MOFs. Following this overview, we now would like to briefly address the question what have we yet learned, and where will the field bring us, thereby identifying main challenges of the field for the near future.

It lies within the nature of a new research field that new synthetic and computational protocols must be defined and verified, thereby pushing the boundaries of science within the respective fields. Consequently, research on defective MOFs, e.g., the synthesis and subsequent characterization and the establishment of structure–property relations, equally challenges experimental and computational chemists.

Experimentalists have now a reasonable toolbox of synthetic techniques that can be applied for incorporating defects into a parent MOF and till today they found many properties, and certainly will find more, that are closely linked to the defect concentration and chemistry. In contrast, the underlying defect structure including local as well as correlated phenomena in MOFs (a prerequisite to establish structure–property relations) is yet barely investigated. Of crucial importance for the development of the research area will be systematic in-depth structural studies that go beyond UiO-66 and involve a standard analysis and characterization procedure on a highest level of accuracy, e.g., the measurement of PXRD, BET surface area, and TGA paired with spectroscopic techniques. A blueprint how such a study can be performed is given by Shearer et al. on the modulation chemistry of UiO-66. Only then we will see if fundamental structure–property relations across different systems will be discovered, or if it will be necessary to look at every system independently. At the same time, the application of currently nonstandard characterization methods such as neutron diffraction,<sup>[152]</sup> anomalous diffraction,<sup>[14]</sup> or PALS are expected to provide a great deal of useful information in the future. For instance, when studying catalysis on a CUS within the framework, the catalytic activity crucially depends on the number and spatial distribution of active sites as well as the presence of diffusion limits. Furthermore, the potential of studying the pore size distribution in situ during synthesis via PALS is promising and opens the opportunity in accessing reaction kinetics in dependency of many parameters, such as temperature, modulator, and so on. More generally, we can summarize that the vast number of different parameters that impact the properties of an MOF, such as linker defects, node defects, heterogeneity, and in turn the detailed structure of the defective systems, is of tremendous importance and challenges experimental scientists in finding and establishing fundamental trends. Here, computational studies can provide access to thermodynamic stabilities and support structural investigations of defective systems. The work by Van Speybroeck and co-workers, studying the mechanical response of different defective UiO systems, and the work by Schmid

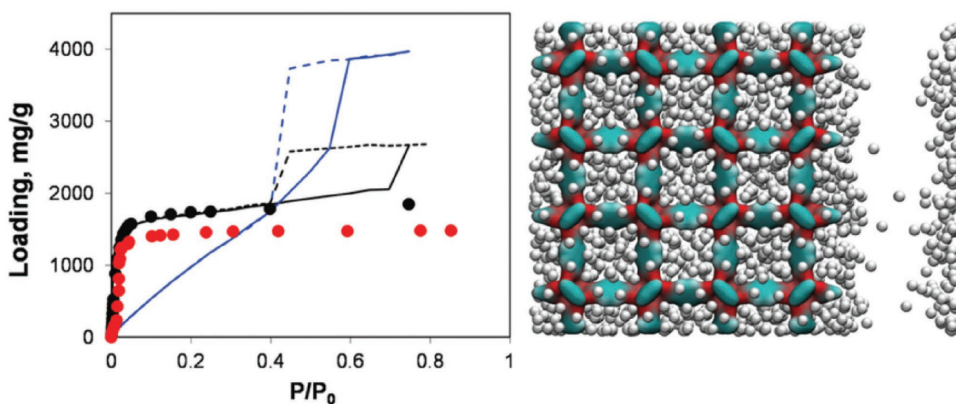


**Figure 20.** Left panel: Adsorption isotherms for argon at 78 K in IRMOF-1. Red symbols are the experimental results,<sup>[146,147]</sup> and black symbols are from molecular simulations for the perfect crystal. Solid and dashed blue lines are adsorption and desorption isotherms, respectively, for the IRMOF-1 structure with 73% of linkers removed as shown in Figure 19. Solid and dashed black lines are for adsorption and desorption isotherms, respectively, for the structure with a 20 Å mesopore. Right panel: Visualization of the state of the system preceding the capillary condensation step. Reproduced with permission.<sup>[116]</sup> Copyright 2016, Royal Chemical Society.



and co-workers on mesopore formation in HKUST-1 induced by clustering of missing node defects are good examples in this context. The success of such kind of computational studies will crucially depend on the interplay with experimental confirmations, hoping for the development of a more rational and theory-guided experimental design in the future.

Going beyond our definition of defects which is focused on the microscopic scale, macroscopic order phenomena of heterogeneous MOFs exhibit exciting opportunities. The challenge is to fully recognize heterogeneity within order as an opportunity of materials design, as highlighted by Yaghi and co-workers in 2015.<sup>[153]</sup> For instance, correlation phenomena of compositional and structural features that contain inherently different functionalities and subsequent domain formation of these depict an exciting opportunity. Such ordering can be seen as a conceptual link between ordering phenomena of missing node defects (mesopore formation) with the formation of domains of different physical and chemical properties. The combination of microscopic with mesoscopic defects, and in particular their interplay, holds promise for dimensions of advanced materials functional design. One example of progress in this direction is the area of flexible and stimuli responsive MOFs on which the effects of defects are now being realized to similarly impact the property.<sup>[154]</sup> For instance, the potential to tune flexible behavior via defect incorporation, e.g., the threshold pressure of an external gas or temperature on which the system becomes flexible, is intriguing. Since such flexibility in MOFs is based upon a balance of enthalpic interactions and entropy, defects that formally increase the configurational entropy of a system are expected to have a large influence. Notably, as early as in 2004 Kitagawa et al. emphasized MOFs being a unique kind of functional soft porous crystals.<sup>[155,156]</sup> It appears now that flexible and stimuli responsive properties of MOFs are intrinsically linked with defects and disorder. Furthermore, defects seem to play a mechanistic key role in synthetic methods being important for advanced MOF design such as postsynthetic modification including solvent-assisted linker and metal ion exchange. The ultimate goal will be to set up and develop a toolbox for knowledge-based MOF defect engineering, and hence the optimization of a material for a certain purpose, e.g., to be used as a catalyst or for CWAs. There is, however, still a long way to go but the progress made over the past two years is promising. At this point, we are in the position to answer the question “Challenge or Opportunity?” raised by Sholl and Lively,<sup>[15]</sup> with the area of defective MOFs bearing many opportunities that not only contain fascinating promises for the area of materials science, but further advance fundamental knowledge at the same time.

## Acknowledgements

S.D., K.E., and W.H. contributed equally to this work. This work was funded by the European Union's Horizon 2020 research and innovation program under the Marie Skłodowska-Curie grant agreement no. 641887 (project acronym: DEFNET). G.K. gratefully thanks the Fonds der chemischen Industrie for support through the Liebig-Fellowship scheme. The authors gratefully thank Dr. Andreas Schneemann for designing the ToC image.

## Conflict of Interest

The authors declare no conflict of interest.

## Keywords

catalysis, defects, electrical conductivity, metal-organic frameworks, sorption

Received: August 9, 2017  
Revised: November 6, 2017  
Published online: January 24, 2018

- [1] R. J. D. Tilley, *Defects in Solids*, John Wiley & Sons, Weinheim, Germany **2008**.
- [2] G. Busch, *Eur. J. Phys.* **1989**, *10*, 254.
- [3] J. L. Tallon, C. Bernhard, H. Shaked, R. L. Hitterman, J. D. Jorgensen, *Phys. Rev. B* **1995**, *51*, 12911.
- [4] A. K. Cheetham, V. E. F. Fender, R. I. Taylor, *J. Phys. C* **1971**, *4*, 2160.
- [5] J. S. Anderson, B. G. Hyde, *J. Phys. Chem. Solids* **1967**, *28*, 1393.
- [6] Z. Fang, B. Bueken, D. E. De Vos, R. A. Fischer, *Angew. Chem., Int. Ed.* **2015**, *54*, 7234.
- [7] W. M. Bloch, A. Burgun, C. J. Coghlan, R. Lee, M. L. Coote, C. J. Doonan, C. J. Sumby, *Nat. Chem.* **2014**, *6*, 906.
- [8] E. A. Kapustin, S. Lee, A. S. Alshammari, O. M. Yaghi, *ACS Cent. Sci.* **2017**, *3*, 662.
- [9] L. Öhrström, *ACS Cent. Sci.* **2017**, *3*, 528.
- [10] O. M. Yaghi, M. O'Keeffe, N. W. Ockwig, H. K. Chae, M. Eddaoudi, J. Kim, *Nature* **2003**, *423*, 705.
- [11] K. T. Butler, A. Walsh, A. K. Cheetham, G. Kieslich, *Chem. Sci.* **2016**, *7*, 6316.
- [12] T. D. Bennett, A. K. Cheetham, A. H. Fuchs, F.-X. Coudert, *Nat. Chem.* **2017**, *9*, 11.
- [13] O. Halbherr, R. A. Fischer, in *The Chemistry of Metal-Organic Frameworks*, (Ed.: S. Kaskel), John Wiley & Sons, Weinheim, Germany **2016**.
- [14] M. J. Cliffe, W. Wan, X. Zou, P. A. Chater, A. K. Kleppe, M. G. Tucker, H. Wilhelm, N. P. Funnell, F.-X. Coudert, A. L. Goodwin, *Nat. Commun.* **2014**, *5*, 4176.
- [15] D. S. Sholl, R. P. Lively, *J. Phys. Chem. Lett.* **2015**, *6*, 3437.
- [16] C. H. Hendon, A. Walsh, *Chem. Sci.* **2015**, *6*, 3674.
- [17] G. C. Shearer, S. Chavan, S. Bordiga, S. Svelle, U. Olsbye, K. P. Lillerud, *Chem. Mater.* **2016**, *28*, 3749.
- [18] J. Canivet, S. Aguado, Y. Schuurman, D. Farrusseng, *J. Am. Chem. Soc.* **2013**, *135*, 4195.
- [19] S. Dissegna, R. Hardian, K. Epp, G. Kieslich, M.-V. Coulet, P. Llewellyn, R. A. Fischer, *CrystEngComm* **2017**, *19*, 4137.
- [20] R. Schlögl, *Angew. Chem., Int. Ed.* **2015**, *54*, 3465.
- [21] Q. Xia, Z. Li, C. Tan, Y. Liu, W. Gong, Y. Cui, *J. Am. Chem. Soc.* **2017**, *139*, 8259.
- [22] T. Islamoglu, S. Goswami, Z. Li, A. J. Howarth, O. K. Farha, J. T. Hupp, *Acc. Chem. Res.* **2017**, *50*, 805.
- [23] S. M. J. Rogge, J. Wieme, L. Vanduyfhuys, S. Vandenbrande, G. Maurin, T. Verstraelen, M. Waroquier, V. Van Speybroeck, *Chem. Mater.* **2016**, *28*, 5721.
- [24] U. Ravon, M. Savonnet, S. Aguado, M. E. Domine, E. Janneau, D. Farrusseng, *Microporous Mesoporous Mater.* **2010**, *129*, 319.
- [25] O. Kozachuk, I. Luz, F. X. Llabrés i Xamena, H. Noei, M. Kauer, H. B. Albada, E. D. Bloch, B. Marler, Y. Wang, M. Muhler, R. A. Fischer, *Angew. Chem., Int. Ed.* **2014**, *53*, 7058.



- [26] F. Vermoortele, B. Bueken, G. Le Bars, B. Van de Voorde, M. Vandichel, K. Houthoofd, A. Vimont, M. Daturi, M. Waroquier, V. Van Speybroeck, C. Kirschhock, D. E. De Vos, *J. Am. Chem. Soc.* **2013**, *135*, 11465.
- [27] S. Marx, W. Kleist, A. Baiker, *J. Catal.* **2011**, *281*, 76.
- [28] F. X. Llabrés i Xamena, F. G. Cirujano, A. Corma, *Microporous Mesoporous Mater.* **2012**, *157*, 112.
- [29] F. Vermoortele, R. Ameloot, L. Alaerts, R. Mattheessen, B. Carlier, E. V. R. Fernandez, J. Gascon, F. Kapteijn, D. E. De Vos, *J. Mater. Chem.* **2012**, *22*, 10313.
- [30] R. J. Marshall, R. S. Forgan, *Eur. J. Inorg. Chem.* **2016**, *2016*, 4310.
- [31] O. Karagiari, M. B. Lalonde, W. Bury, A. A. Sarjeant, O. K. Farha, J. T. Hupp, *J. Am. Chem. Soc.* **2012**, *134*, 18790.
- [32] O. Karagiari, W. Bury, J. E. Mondloch, J. T. Hupp, O. K. Farha, *Angew. Chem., Int. Ed.* **2014**, *53*, 4530.
- [33] O. Karagiari, N. A. Vermeulen, R. C. Klet, T. C. Wang, P. Z. Moghadam, S. S. Al-Juaid, J. F. Stoddart, J. T. Hupp, O. K. Farha, *Inorg. Chem.* **2015**, *54*, 1785.
- [34] S. J. Lee, C. Doussot, A. Baux, L. Liu, G. B. Jameson, C. Richardson, J. J. Pak, F. Trousselet, F.-X. Coudert, S. G. Telfer, *Chem. Mater.* **2016**, *28*, 368.
- [35] P. Deria, J. E. Mondloch, E. Tylianakis, P. Ghosh, W. Bury, R. Q. Snurr, J. T. Hupp, O. K. Farha, *J. Am. Chem. Soc.* **2013**, *135*, 16801.
- [36] G. C. Shearer, S. Chavan, J. Ethiraj, J. G. Vitillo, S. Svelle, U. Olsbye, C. Lamberti, S. Bordiga, K. P. Lillerud, *Chem. Mater.* **2014**, *26*, 4068.
- [37] S. Gadipelli, Z. Guo, *Chem. Mater.* **2014**, *26*, 6333.
- [38] T. D. Bennett, T. K. Todorova, E. F. Baxter, D. G. Reid, C. Gervais, B. Bueken, B. Van de Voorde, D. De Vos, D. A. Keen, C. Mellot-Draznieks, *Phys. Chem. Chem. Phys.* **2016**, *18*, 2192.
- [39] C. Atzori, G. C. Shearer, L. Maschio, B. Civalieri, F. Bonino, C. Lamberti, S. Svelle, K. P. Lillerud, S. Bordiga, *J. Phys. Chem. C* **2017**, *121*, 9312.
- [40] Y. Wang, W. Zhang, X. Wu, C. Luo, Q. Wang, J. Li, L. Hu, *Synth. Met.* **2017**, *228*, 18.
- [41] K. Sethi, S. Sharma, I. Roy, *RSC Adv.* **2016**, *6*, 76861.
- [42] Y. Du, R. Z. Chen, J. F. Yao, H. T. Wang, *J. Alloys Compd.* **2013**, *551*, 125.
- [43] M. Liu, A. G. Wong-Foy, R. S. Vallery, W. E. Frieze, J. K. Schnobrich, D. W. Gidley, A. J. Matzger, *Adv. Mater.* **2010**, *22*, 1598.
- [44] J. I. Feldblyum, M. Liu, D. W. Gidley, A. J. Matzger, *J. Am. Chem. Soc.* **2011**, *133*, 18257.
- [45] S. S. Mondal, S. Dey, A. G. Attallah, A. Bhunia, A. Kelling, U. Schilde, R. Krause-Rehberg, C. Janiak, H.-J. Holdt, *ChemistrySelect* **2016**, *1*, 4320.
- [46] A. W. Thornton, K. E. Jelfs, K. Konstas, C. M. Doherty, A. J. Hill, A. K. Cheetham, T. D. Bennett, *Chem. Commun.* **2016**, *52*, 3750.
- [47] R. C. Klet, Y. Liu, T. C. Wang, J. T. Hupp, O. K. Farha, *J. Mater. Chem. A* **2016**, *4*, 1479.
- [48] Y. Liu, R. C. Klet, J. T. Hupp, O. Farha, *Chem. Commun.* **2016**, *52*, 7806.
- [49] L. Valenzano, B. Civalieri, S. Chavan, S. Bordiga, M. H. Nilsen, S. Jakobsen, K. P. Lillerud, C. Lamberti, *Chem. Mater.* **2011**, *23*, 1700.
- [50] J. Canivet, A. Fateeva, Y. Guo, B. Coasne, D. Farrusseng, *Chem. Soc. Rev.* **2014**, *43*, 5594.
- [51] P. Küsgens, M. Rose, I. Senkovska, H. Fröde, A. Henschel, S. Siegle, S. Kaskel, *Microporous Mesoporous Mater.* **2009**, *120*, 325.
- [52] W. Zhang, M. Kauer, O. Halbherr, K. Epp, P. Guo, M. I. Gonzalez, D. J. Xiao, C. Wiktor, F. X. Llabrés i Xamena, C. Wöll, Y. Wang, M. Muhler, R. A. Fischer, *Chem. Eur. J.* **2016**, *22*, 14297.
- [53] F. G. Cirujano, A. Corma, F. X. Llabrés i Xamena, *Chem. Eng. Sci.* **2015**, *124*, 52.
- [54] G. Cai, H.-L. Jiang, *Angew. Chem., Int. Ed.* **2017**, *56*, 563.
- [55] P. Á. Szilágyi, P. Serra-Crespo, J. Gascon, H. Geerlings, B. Dam, *Front. Energy Res.* **2016**, *4*.
- [56] K. Behrens, S. S. Mondal, R. Nöske, I. A. Baburin, S. Leoni, C. Günter, J. Weber, H.-J. Holdt, *Inorg. Chem.* **2015**, *54*, 10073.
- [57] L. M. Rodríguez-Albelo, E. López-Maya, S. Hamad, A. R. Ruiz-Salvador, S. Calero, J. A. R. Navarro, *Nat. Commun.* **2017**, *8*, 14457.
- [58] A. X. Lu, M. McEntee, M. A. Browe, M. G. Hall, J. B. DeCoste, G. W. Peterson, *ACS Appl. Mater. Interfaces* **2017**, *9*, 13632.
- [59] A. M. Plonka, Q. Wang, W. O. Gordon, A. Balboa, D. Troya, W. Guo, C. H. Sharp, S. D. Senanayake, J. R. Morris, C. L. Hill, A. I. Frenkel, *J. Am. Chem. Soc.* **2017**, *139*, 599.
- [60] B. Li, X. Zhu, K. Hu, Y. Li, J. Feng, J. Shi, J. Gu, *J. Hazard. Mater.* **2016**, *302*, 57.
- [61] T. Islamoglu, A. Atilgan, S.-Y. Moon, G. W. Peterson, J. B. DeCoste, M. Hall, J. T. Hupp, O. K. Farha, *Chem. Mater.* **2017**, *29*, 2672.
- [62] S.-Y. Moon, E. Proussaloglou, G. W. Peterson, J. B. DeCoste, M. G. Hall, A. J. Howarth, J. T. Hupp, O. K. Farha, *Chem. Eur. J.* **2016**, *22*, 14864.
- [63] P. Li, S.-Y. Moon, M. A. Guelta, S. P. Harvey, J. T. Hupp, O. K. Farha, *J. Am. Chem. Soc.* **2016**, *138*, 8052.
- [64] Y. Liu, A. J. Howarth, J. T. Hupp, O. K. Farha, *Angew. Chem., Int. Ed.* **2015**, *54*, 9001.
- [65] E. López-Maya, C. Montoro, L. M. Rodríguez-Albelo, S. D. Aznar Cervantes, A. A. Lozano-Pérez, J. L. Cenis, E. Barea, J. A. R. Navarro, *Angew. Chem., Int. Ed.* **2015**, *54*, 6790.
- [66] I. Cortinas, J. A. Field, M. Kopplin, J. R. Garbarino, A. J. Gandolfi, R. Sierra-Alvarez, *Environ. Sci. Technol.* **2006**, *40*, 2951.
- [67] G. L. Baughman, E. J. Weber, *Environ. Sci. Technol.* **1994**, *28*, 267.
- [68] K. Fan, W.-X. Nie, L.-P. Wang, C.-H. Liao, S.-S. Bao, L.-M. Zheng, *Chem. Eur. J.* **2017**, *23*, 6615.
- [69] C. A. Fernandez, S. K. Nune, H. V. Annapureddy, L. X. Dang, B. P. McGrail, F. Zheng, E. Polikarpov, D. L. King, C. Freeman, K. P. Brooks, *Dalton Trans.* **2015**, *44*, 13490.
- [70] Y.-B. Huang, M. Shen, X. Wang, P. Huang, R. Chen, Z.-J. Lin, R. Cao, *J. Catal.* **2016**, *333*, 1.
- [71] L. Sun, M. G. Campbell, M. Dincă, *Angew. Chem., Int. Ed.* **2016**, *55*, 3566.
- [72] I. Stassen, N. Burtch, A. Talin, P. Falcaro, M. Allendorf, R. Ameloot, *Chem. Soc. Rev.* **2017**, *46*, 3185.
- [73] S. R. Ahrenholtz, C. C. Epley, A. J. Morris, *J. Am. Chem. Soc.* **2014**, *136*, 2464.
- [74] T. Kambe, R. Sakamoto, K. Hoshiko, K. Takada, M. Miyachi, J.-H. Ryu, S. Sasaki, J. Kim, K. Nakazato, M. Takata, H. Nishihara, *J. Am. Chem. Soc.* **2013**, *135*, 2462.
- [75] T. Kambe, R. Sakamoto, T. Kusamoto, T. Pal, N. Fukui, K. Hoshiko, T. Shimojima, Z. Wang, T. Hirahara, K. Ishizaka, S. Hasegawa, F. Liu, H. Nishihara, *J. Am. Chem. Soc.* **2014**, *136*, 14357.
- [76] D. Sheberla, L. Sun, M. A. Blood-Forsythe, S. Er, C. R. Wade, C. K. Brozek, A. Aspuru-Guzik, M. Dincă, *J. Am. Chem. Soc.* **2014**, *136*, 8859.
- [77] D. Sheberla, J. C. Bachman, J. S. Elias, C.-J. Sun, Y. Shao-Horn, M. Dinca, *Nat. Mater.* **2017**, *16*, 220.
- [78] S. S. Park, E. R. Hontz, L. Sun, C. H. Hendon, A. Walsh, T. Van Voorhis, M. Dincă, *J. Am. Chem. Soc.* **2015**, *137*, 1774.
- [79] L. Sun, S. S. Park, D. Sheberla, M. Dincă, *J. Am. Chem. Soc.* **2016**, *138*, 14772.
- [80] L. Sun, C. H. Hendon, M. A. Minier, A. Walsh, M. Dincă, *J. Am. Chem. Soc.* **2015**, *137*, 6164.
- [81] A. R. Blythe, D. Bloor, *Electrical Properties of Polymers*, Cambridge University Press, New York **2005**.
- [82] A. W. Hains, Z. Liang, M. A. Woodhouse, B. A. Gregg, *Chem. Rev.* **2010**, *110*, 6689.
- [83] C. Wang, H. Dong, W. Hu, Y. Liu, D. Zhu, *Chem. Rev.* **2012**, *112*, 2208.

- [84] C. K. Chiang, C. R. Fincher, Y. W. Park, A. J. Heeger, H. Shirakawa, E. J. Louis, S. C. Gau, A. G. MacDiarmid, *Phys. Rev. Lett.* **1977**, 39, 1098.
- [85] Y. Kobayashi, B. Jacobs, M. D. Allendorf, J. R. Long, *Chem. Mater.* **2010**, 22, 4120.
- [86] H.-Y. Wang, J.-Y. Ge, C. Hua, C.-Q. Jiao, Y. Wu, C. F. Leong, D. M. D'Alessandro, T. Liu, J.-L. Zuo, *Angew. Chem., Int. Ed.* **2017**, 56, 5465.
- [87] K. J. Erickson, F. Léonard, V. Stavila, M. E. Foster, C. D. Spataru, R. E. Jones, B. M. Foley, P. E. Hopkins, M. D. Allendorf, A. A. Talin, *Adv. Mater.* **2015**, 27, 3453.
- [88] A. A. Talin, A. Centrone, A. C. Ford, M. E. Foster, V. Stavila, P. Haney, R. A. Kinney, V. Szalai, F. El Gabaly, H. P. Yoon, F. Léonard, M. D. Allendorf, *Science* **2014**, 343, 66.
- [89] M. D. Allendorf, M. E. Foster, F. Léonard, V. Stavila, P. L. Feng, F. P. Doty, K. Leong, E. Y. Ma, S. R. Johnston, A. A. Talin, *J. Phys. Chem. Lett.* **2015**, 6, 1182.
- [90] A. Sengupta, S. Datta, C. Su, T. S. Herng, J. Ding, J. J. Vittal, K. P. Loh, *ACS Appl. Mater. Interfaces* **2016**, 8, 16154.
- [91] V. Stavila, C. Schneider, C. Mowry, T. R. Zeitler, J. A. Greathouse, A. L. Robinson, J. M. Denning, J. Volponi, K. Leong, W. Quan, M. Tu, R. A. Fischer, M. D. Allendorf, *Adv. Funct. Mater.* **2016**, 26, 1699.
- [92] M. D. Allendorf, R. Medishetty, R. A. Fischer, *MRS Bull.* **2016**, 41, 865.
- [93] A. M. Ullman, J. W. Brown, M. E. Foster, F. Léonard, K. Leong, V. Stavila, M. D. Allendorf, *Inorg. Chem.* **2016**, 55, 7233.
- [94] H. Shiozawa, B. C. Bayer, H. Peterlik, J. C. Meyer, W. Lang, T. Pichler, *Sci. Rep.* **2017**, 7, 2439.
- [95] M. D. Allendorf, A. Schwartzberg, V. Stavila, A. A. Talin, *Chem. Eur. J.* **2011**, 17, 11372.
- [96] K.-D. Kreuer, *Chem. Mater.* **1996**, 8, 610.
- [97] S. Horike, D. Umeyama, S. Kitagawa, *Acc. Chem. Res.* **2013**, 46, 2376.
- [98] T. Yamada, K. Otsubo, R. Makiura, H. Kitagawa, *Chem. Soc. Rev.* **2013**, 42, 6655.
- [99] V. G. Ponomareva, K. A. Kovalenko, A. P. Chupakhin, D. N. Dybtsev, E. S. Shutova, V. P. Fedin, *J. Am. Chem. Soc.* **2012**, 134, 15640.
- [100] M. G. Goesten, J. Juan-Alcañiz, E. V. Ramos-Fernandez, K. B. Sai Sankar Gupta, E. Stavitski, H. van Bekkum, J. Gascon, F. Kapteijn, *J. Catal.* **2011**, 281, 177.
- [101] H. O kawa, M. Sadakiyo, T. Yamada, M. Maesato, M. Ohba, H. Kitagawa, *J. Am. Chem. Soc.* **2013**, 135, 2256.
- [102] J. M. Taylor, S. Dekura, R. Ikeda, H. Kitagawa, *Chem. Mater.* **2015**, 27, 2286.
- [103] J. M. Taylor, T. Komatsu, S. Dekura, K. Otsubo, M. Takata, H. Kitagawa, *J. Am. Chem. Soc.* **2015**, 137, 11498.
- [104] M. Sadakiyo, H. Kasai, K. Kato, M. Takata, M. Yamauchi, *J. Am. Chem. Soc.* **2014**, 136, 1702.
- [105] C. Montoro, P. Ocón, F. Zamora, J. A. R. Navarro, *Chem. Eur. J.* **2016**, 22, 1646.
- [106] S. Tominaka, A. K. Cheetham, *RSC Adv.* **2014**, 4, 54382.
- [107] N. E. A. El-Gamel, *Eur. J. Inorg. Chem.* **2015**, 2015, 1351.
- [108] D. Wu, W. Yan, H. Xu, E. Zhang, Q. Li, *Inorg. Chim. Acta* **2017**, 460, 93.
- [109] K. D. Vogiatzis, E. Haldoupis, D. J. Xiao, J. R. Long, J. I. Siepmann, L. Gagliardi, *J. Phys. Chem. C* **2016**, 120, 18707.
- [110] W. Zhang, M. Kauer, P. Guo, S. Kunze, S. Cwik, M. Muhler, Y. Wang, K. Epp, G. Kieslich, R. A. Fischer, *Eur. J. Inorg. Chem.* **2017**, 2017, 925.
- [111] J. P. Dürholt, J. Keupp, Schmid, Rochus, *Eur. J. Inorg. Chem.* **2016**, 2016, 4517.
- [112] J. Bentley, G. S. Foo, M. Rungta, N. Sangar, C. Sievers, D. S. Sholl, S. Nair, *Ind. Eng. Chem. Res.* **2016**, 55, 5043.
- [113] B. Liu, Y. Li, S. C. Oh, Y. Fang, H. Xi, *RSC Adv.* **2016**, 6, 61006.
- [114] G. Barin, V. Krungleviciute, O. Gutov, J. T. Hupp, T. Yildirim, O. K. Farha, *Inorg. Chem.* **2014**, 53, 6914.
- [115] T. Lee, Y. H. Chang, H. L. Lee, *CrystEngComm* **2017**, 19, 426.
- [116] L. Sarkisov, *Dalton Trans.* **2016**, 45, 4203.
- [117] Y. Luan, Y. Qi, H. Gao, R. S. Andriamitantoa, N. Zheng, G. Wang, *J. Mater. Chem. A* **2015**, 3, 17320.
- [118] P. Cheng, Y. H. Hu, *Int. J. Energy Res.* **2016**, 40, 846.
- [119] Z. Hu, Y. Peng, Y. Gao, Y. Qian, S. Ying, D. Yuan, S. Horike, N. Ogiwara, R. Babarao, Y. Wang, N. Yan, D. Zhao, *Chem. Mater.* **2016**, 28, 2659.
- [120] Z. Wang, H. Sezen, J. Liu, C. Yang, S. E. Roggenbuck, K. Peikert, M. Fröba, A. Mavrandonakis, B. Supronowicz, T. Heine, H. Gliemann, C. Wöll, *Microporous Mesoporous Mater.* **2015**, 207, 53.
- [121] S. Ling, B. Slater, *Chem. Sci.* **2016**, 7, 4706.
- [122] W. Liang, C. J. Coghlan, F. Ragon, M. Rubio-Martinez, D. M. D'Alessandro, R. Babarao, *Dalton Trans.* **2016**, 45, 4496.
- [123] J. N. Joshi, E. Y. Garcia-Gutierrez, C. M. Moran, J. I. Deneff, K. S. Walton, *J. Phys. Chem. C* **2017**, 121, 3310.
- [124] Z. Hu, S. Faucher, Y. Zhuo, Y. Sun, S. Wang, D. Zhao, *Chem. Eur. J.* **2015**, 21, 17246.
- [125] G. C. Shearer, J. G. Vitillo, S. Bordiga, S. Svelle, U. Olsbye, K. P. Lillerud, *Chem. Mater.* **2016**, 28, 7190.
- [126] D. Yang, V. Bernales, T. Islamoglu, O. K. Farha, J. T. Hupp, C. J. Cramer, L. Gagliardi, B. C. Gates, *J. Am. Chem. Soc.* **2016**, 138, 15189.
- [127] A. W. Thornton, R. Babarao, A. Jain, F. Trousselet, F. X. Coudert, *Dalton Trans.* **2016**, 45, 4352.
- [128] C. A. Trickett, K. J. Gagnon, S. Lee, F. Gándara, H.-B. Bürgi, O. M. Yaghi, *Angew. Chem., Int. Ed.* **2015**, 54, 11162.
- [129] M. Vandichel, J. Hajek, A. Ghysels, A. De Vos, M. Waroquier, V. Van Speybroeck, *CrystEngComm* **2016**, 18, 7056.
- [130] P. Ghosh, Y. J. Colon, R. Q. Snurr, *Chem. Comm.* **2014**, 50, 11329.
- [131] A. De Vos, K. Hendrickx, P. Van Der Voort, V. Van Speybroeck, K. Lejaeghere, *Chem. Mater.* **2017**, 29, 3006.
- [132] J. K. Bristow, K. L. Svane, D. Tian, J. M. Skelton, J. D. Gale, A. Walsh, *J. Phys. Chem. C* **2016**, 120, 9276.
- [133] M. J. Cliffe, J. A. Hill, C. A. Murray, F.-X. Coudert, A. L. Goodwin, *Phys. Chem. Chem. Phys.* **2015**, 17, 11586.
- [134] O. V. Gutov, M. G. Hevia, E. C. Escudero-Adán, A. Shafir, *Inorg. Chem.* **2015**, 54, 8396.
- [135] M. J. Cliffe, E. Castillo-Martínez, Y. Wu, J. Lee, A. C. Forse, F. C. N. Firth, P. Z. Moghadam, D. Fairen-Jimenez, M. W. Gaultois, J. A. Hill, O. V. Magdysyuk, B. Slater, A. L. Goodwin, C. P. Grey, *J. Am. Chem. Soc.* **2017**, 139, 5397.
- [136] C. Zhang, C. Han, D. S. Sholl, J. R. Schmidt, *J. Phys. Chem. Lett.* **2016**, 7, 459.
- [137] M. J. Lee, H. T. Kwon, H.-K. Jeong, *J. Membr. Sci.* **2017**, 529, 105.
- [138] H. T. Kwon, H.-K. Jeong, A. S. Lee, H. S. An, T. Lee, E. Jang, J. S. Lee, J. Choi, *Chem. Commun.* **2016**, 52, 11669.
- [139] R. Han, D. S. Sholl, *J. Phys. Chem. C* **2016**, 120, 27380s.
- [140] R. Semino, N. A. Ramsahye, A. Ghoufi, G. Maurin, *Microporous Mesoporous Mater.* **2017**, 254, 184.
- [141] J. Ren, N. M. Musyoka, H. W. Langmi, B. C. North, M. Mathe, W. Pang, M. Wang, J. Walker, *Appl. Surf. Sci.* **2017**, 404, 263.
- [142] J. Canivet, M. Vandichel, D. Farrusseng, *Dalton Trans.* **2016**, 45, 4090.
- [143] H. Fei, J. F. Cahill, K. A. Prather, S. M. Cohen, *Inorg. Chem.* **2013**, 52, 4011.
- [144] P. Deria, J. E. Mondloch, O. Karagiari, W. Bury, J. T. Hupp, O. K. Farha, *Chem. Soc. Rev.* **2014**, 43, 5896.
- [145] Z. Wang, S. M. Cohen, *Chem. Soc. Rev.* **2009**, 38, 1315.

- [146] H. Li, M. Eddaoudi, M. O'Keeffe, O. M. Yaghi, *Nature* **1999**, *402*, 276.
- [147] D. Dubbeldam, H. Frost, K. S. Walton, R. Q. Snurr, *FFE* **2007**, *261*, 152.
- [148] Z. Fang, J. P. Dürholt, M. Kauer, W. Zhang, C. Lochenie, B. Jee, B. Albada, N. Metzler-Nolte, A. Pöpl, B. Weber, M. Muhler, Y. Wang, R. Schmid, R. A. Fischer, *J. Am. Chem. Soc.* **2014**, *136*, 9627.
- [149] J. P. Durholt, R. Galvelis, R. Schmid, *Dalton Trans.* **2016**, *45*, 4370.
- [150] S. Bureekaew, V. Balwani, S. Amirjalayer, R. Schmid, *CrystEngComm* **2015**, *17*, 344.
- [151] D. Yang, S. O. Odoh, T. C. Wang, O. K. Farha, J. T. Hupp, C. J. Cramer, L. Gagliardi, B. C. Gates, *J. Am. Chem. Soc.* **2015**, *137*, 7391.
- [152] H. Wu, Y. S. Chua, V. Krungleviciute, M. Tyagi, P. Chen, T. Yildirim, W. Zhou, *J. Am. Chem. Soc.* **2013**, *135*, 10525.
- [153] H. Furukawa, U. Müller, O. M. Yaghi, *Angew. Chem., Int. Ed.* **2015**, *54*, 3417.
- [154] M. Mendt, F. Gutt, N. Kavoosi, V. Bon, I. Senkovska, S. Kaskel, A. Pöpl, *J. Phys. Chem. C* **2016**, *120*, 14246.
- [155] S. Horike, S. Shimomura, S. Kitagawa, *Nat. Chem.* **2009**, *1*, 695.
- [156] S. Kitagawa, R. Kitaura, S.-i. Noro, *Angew. Chem., Int. Ed.* **2004**, *43*, 2334.